

CADM1 Expression and Stepwise Downregulation of CD7 Are Closely Associated with Clonal Expansion of HTLV-I-Infected Cells in Adult T-cell Leukemia/Lymphoma

Seiichiro Kobayashi¹, Kazumi Nakano⁵, Eri Watanabe², Tomohiro Ishigaki², Nobuhiro Ohno³, Koichiro Yuji³, Naoki Oyaizu⁴, Satomi Asanuma⁵, Makoto Yamagishi⁵, Tadanori Yamochi⁵, Nobukazu Watanabe², Arinobu Tojo^{1,3}, Toshiki Watanabe⁵, and Kaoru Uchamaru³

Abstract

Purpose: Cell adhesion molecule 1 (CADM1), initially identified as a tumor suppressor gene, has recently been reported to be ectopically expressed in primary adult T-cell leukemia-lymphoma (ATL) cells. We incorporated CADM1 into flow-cytometric analysis to reveal oncogenic mechanisms in human T-cell lymphotropic virus type I (HTLV-I) infection by purifying cells from the intermediate stages of ATL development.

Experimental Design: We isolated CADM1- and CD7-expressing peripheral blood mononuclear cells of asymptomatic carriers and ATLS using multicolor flow cytometry. Fluorescence-activated cell sorted (FACS) subpopulations were subjected to clonal expansion and gene expression analysis.

Results: HTLV-I-infected cells were efficiently enriched in CADM1⁺ subpopulations (D, CADM1^{pos}CD7^{dim} and N, CADM1^{pos}CD7^{neg}). Clonally expanding cells were detected exclusively in these subpopulations in asymptomatic carriers with high proviral load, suggesting that the appearance of D and N could be a surrogate marker of progression from asymptomatic carrier to early ATL. Further disease progression was accompanied by an increase in N with a reciprocal decrease in D, indicating clonal evolution from D to N. The gene expression profiles of D and N in asymptomatic carriers showed similarities to those of indolent ATLS, suggesting that these subpopulations represent premalignant cells. This is further supported by the molecular hallmarks of ATL, that is, drastic downregulation of miR-31 and upregulation of abnormal *Helios* transcripts.

Conclusion: The CADM1 versus CD7 plot accurately reflects disease progression in HTLV-I infection, and CADM1⁺ cells with downregulated CD7 in asymptomatic carriers have common properties with those in indolent ATLS. *Clin Cancer Res*; 20(11); 2851–61. ©2014 AACR.

Introduction

Human T-cell lymphotropic virus type I (HTLV-I) is a human retrovirus that causes HTLV-I-associated diseases, such as adult T-cell leukemia-lymphoma (ATL), HTLV-I-associated myelopathy/tropical spastic paraparesis, and HTLV-I uveitis (1–3). In Japan, the estimated lifetime risk of developing ATL in HTLV-I carriers is 6% to 7% for males

and 2% to 3% for females (4–6). It takes several decades for HTLV-I-infected cells to reach the final stage of multistep oncogenesis, which is clinically recognized as aggressive ATL (acute-type and lymphoma-type; ref. 7). Molecular interaction of viral genes [e.g., Tax and the HTLV-I basic leucine zipper (HBZ) gene] with the cellular machinery causes various genetic and epigenetic alterations (7–11). However, difficulties in purifying HTLV-I-infected cells *in vivo* seem to have hindered understanding of the genetic events that are directly involved in the multistep oncogenesis of ATL.

Upregulation or aberrant expression of cell surface markers, such as CCR4 and CD25, is useful for diagnosis of ATL and has been utilized for molecular-targeted therapy (12, 13). However, the expression levels of these markers vary among patients, which often make it difficult to identify ATL cells specifically based on the immunophenotype. Previously, we focused on downregulated markers in acute-type ATL cells, such as CD3 and CD7, and successfully purified ATL cells using the CD3 versus CD7 plot of CD4⁺ cells (14). Analysis of other clinical subtypes

Authors' affiliations: ¹Division of Molecular Therapy; ²Laboratory of Diagnostic Medicine, Division of Stem Cell Therapy; ³Department of Hematology/Oncology, Research Hospital; ⁴Clinical Laboratory, Research Hospital, Institute of Medical Science; and ⁵Graduate School of Frontier Sciences, The University of Tokyo, Tokyo, Japan

Note: Supplementary data for this article are available at Clinical Cancer Research Online (<http://clincancerres.aacrjournals.org/>).

Corresponding Author: Kaoru Uchamaru, Institute of Medical Science, The University of Tokyo, 4-6-1 Shirokanedai, Minato-ku, Tokyo 108-8639, Japan. Phone: 81-3-5449-5542; Fax: 81-3-5449-5429; E-mail: uchamaru@ims.u-tokyo.ac.jp

doi: 10.1158/1078-0432.CCR-13-3169

©2014 American Association for Cancer Research.

Translational Relevance

In this study, we showed that the cell adhesion molecule 1 (CADM1) versus CD7 plot reflects the progression of disease in patients infected with human T-cell lymphotropic virus type I (HTLV-I), in that the proportion of CADM1⁺ subpopulations (D, CADM1^{pos}CD7^{dim} and N, CADM1^{pos}CD7^{neg}) increased with the progression from HTLV-I asymptomatic carrier (AC) to indolent adult T-cell leukemia-lymphoma (ATL) to aggressive ATL. We confirmed the purity of the clonal HTLV-I-infected cells in these subpopulations of various clinical subtypes, including asymptomatic carriers. The results from the flow-cytometric analysis will help physicians assess disease status. The analysis is also practical in screening for putative high-risk HTLV-I asymptomatic carriers, which show nearly identical flow-cytometric and gene expression profiles with those of smoldering-type ATL patients. Furthermore, cell sorting by flow cytometry enables purification of clonally expanding cells in various stages of oncogenesis in the course of progression to aggressive ATL. Detailed molecular analysis of these cells will provide valuable information about the molecular events involved in multistep oncogenesis of ATL.

(indolent ATLs and HTLV-I asymptomatic carriers; AC) revealed that HTLV-I-infected and clonally expanded cells were purified similarly and that the subpopulations with downregulated CD7 grew concomitantly with the progression of HTLV-I infection (15). Although this type of flow-cytometric analysis was shown to be a useful tool, a substantial subpopulation of T cells shows downregulated expression of CD7 under physiologic (16, 17) and certain pathologic conditions, including autoimmune disorders, viral infection, and hematopoietic stem cell transplantation (18–23).

Recently, Sasaki and colleagues reported ectopic overexpression of the cell adhesion molecule 1/tumor suppressor in lung cancer 1 (CADM1/TSLC1) gene in primary acute-type ATL cells based on expression profile analysis (24, 25). CADM1 (/TSLC1) is a cell-adhesion molecule that was originally identified as a tumor suppressor in lung cancers (25, 26). In addition, numbers of CD4⁺ CADM1⁺ cells have been found to be significantly correlated with the proviral load (PVL) in both ATLs and HTLV-I asymptomatic carriers (25, 27). Thus, CADM1 is a good candidate marker of HTLV-I-infected cells. In the present study, we incorporated CADM1 into our flow-cytometric analysis. In the CADM1 versus CD7 plot of CD4⁺ cells, HTLV-I-infected and clonally expanded cells were efficiently enriched in the CADM1⁺ subpopulations regardless of disease status. In these cells, stepwise CD7 downregulation (from dimly positive to negative) occurred with disease progression. The proportion of the three subpopulations observed in this plot [P,

CADM1^{negative(neg)}CD7^{positive(pos)}, D, CADM1^{pos}CD7^{dim}, and N, CADM1^{pos}CD7^{neg}] accurately reflected the disease status in HTLV-I infection. The analysis of comprehensive gene expression in each subpopulation revealed that the expression profile of CADM1⁺ subpopulations in indolent ATLs showed similarities with that in asymptomatic carriers with high PVL; yet, it was distinct from that in aggressive ATLs. These D and N subpopulations were indicative of HTLV-I-infected cells in the intermediate stage of ATL development.

Materials and Methods

Cell lines and patient samples

TL-Om1, an HTLV-I-infected cell line (28), was provided by Dr. Sugamura (Tohoku University, Sendai, Japan). The MT-2 cell line was a gift from Dr. Miyoshi (Kochi University, Kochi, Japan) and ST-1 was from Dr. Nagai (Nagasaki University, Nagasaki, Japan). Peripheral blood samples were collected from in-patients and out-patients at our hospital, as described in our previous reports (14, 15). As shown in Supplementary Table S1, 26 cases were analyzed (10 cases of asymptomatic carrier; 5 cases of smoldering-type; 6 cases of chronic-type; and 5 cases of acute-type). All patients with ATL were categorized into clinical subtypes according to Shimoyama's criteria (12, 29). Patients with various complications, such as autoimmune disorders and systemic infections, were excluded. Lymphoma-type patients were also excluded because ATL cells are not considered to exist in the peripheral blood of this clinical subtype. Samples collected from six healthy volunteers (mean age 48.8 years; range 34–66 years) were used as normal controls. The present study was approved by the Institutional Review Board of our institute (the University of Tokyo, Tokyo, Japan). Written informed consent was obtained from all patients and healthy volunteers.

Flow cytometry and cell sorting

Peripheral blood mononuclear cells (PBMC) were isolated from whole blood by density gradient centrifugation, as described previously (14). An unlabeled CADM1 antibody (clone 3E1) and an isotype control chicken immunoglobulin Y (IgY) antibody were purchased from MBL. These were biotinylated (primary amine biotinylation) using biotin N-hydroxysuccinimide ester (Sigma-Aldrich). Pacific Orange-conjugated anti-CD14 antibody was purchased from Caltag-Invitrogen. All other antibodies were obtained from BioLegend. Cells were stained using a combination of biotin-CADM1, allophycocyanin (APC)-CD7, APC-Cy7-CD3, Pacific Blue-CD4, and Pacific Orange-CD14. After washing, phycoerythrin-conjugated streptavidin was applied. Propidium iodide (Sigma-Aldrich) was added to the samples to stain dead cells immediately before flow cytometry. A FACSAria instrument (BD Immunocytometry Systems) was used for all multicolor flow cytometry and fluorescence-activated cell sorting (FACS). Data were analyzed using FlowJo software (TreeStar). The gating

procedure for a representative case is shown in Supplementary Fig. S1.

Quantification of HTLV-I proviral load by real-time quantitative PCR

PVL in FACS-sorted PBMCs was quantified by real-time quantitative PCR (TaqMan method) using the ABI Prism 7000 sequence detection system (Applied Biosystems), as described previously (14, 30).

Evaluation of HTLV-I HBZ gene amplification by semiquantitative PCR

HTLV-I HBZ gene amplification was performed as described previously (25). Briefly, the 25- μ L PCR mixture consisted of 20 pmol of each primer, 2.0 μ L of mixed deoxynucleotide triphosphates (2.5 mmol/L each), 2.5 μ L of $10\times$ PCR buffer, 1.5 μ L of $MgCl_2$ (25 mmol/L), 0.1 μ L of AmpliTaq Gold DNA Polymerase (Applied Biosystems), and 20 ng of DNA extracted from cell lines and clinical samples. The PCR consisted of initial denaturation at 94°C for 9 minutes, 30 cycles of 94°C for 30 seconds, 57°C for 30 seconds, and 72°C for 45 seconds, followed by 72°C for 5 minutes. The β -actin gene (*ACTB*) was used as an internal reference control. The primer sequences used were as follows: HBZ forward, 5'-CGCTGCCGATCACGATG-3'; HBZ reverse, 5'-GGAGGAATTGGTGGACG-3'; ACTB forward, 5'-CGTGCTCAGGGCTTCTT-3'; and ACTB reverse, 5'-TGAA-GGTCTCAAACATGATCTG-3'. Amplification with these pairs of oligonucleotides yielded 177-bp HBZ and 731-bp β -actin fragments.

FISH for quantification of HTLV-I-infected cells

FISH analysis was performed to detect HTLV-I proviral DNA in mononuclear cells that had been FACS-sorted on the basis of the CADM1 versus CD7 plot. These samples were sent to a commercial laboratory (Chromosome Science Labo Inc.), where FISH analysis was performed. Briefly, pUC/HTLV-I plasmid containing the whole-HTLV-I genome was labeled with digoxigenin by the nick translation method, and was then used as a FISH probe. Pretreatment, hybridization, and washing were performed according to standard laboratory protocols. To remove fluorochrome-labeled antibodies attached to the cell surface, pretreatment consisted of treatment with 0.005% pepsin and 0.1 N HCl. The FISH probe was detected with Cy3-labeled anti-digoxigenin antibody. Cells were counterstained with 4', 6 diamidino-2-phenylindole. The results were visualized using a DMRA2 conventional fluorescence microscope (Leica) and photographed using a Leica CW4000 cytogenetics workstation. Hybridization signals were evaluated in approximately 100 nuclei.

Inverse long PCR to assess the clonality of HTLV-I-infected cells

For clonality analysis, inverse long PCR was performed as described previously (14). First, 1 μ g genomic DNA extracted from the FACS-sorted cells was digested with *Pst*I

or *Eco*RI at 37°C overnight. RNase A (Qiagen) was added to remove residual RNA completely. DNA fragments were purified using a QIAEX2 Gel Extraction Kit (Qiagen). The purified DNA was self-ligated with T4 DNA ligase (Takara Bio) at 16°C overnight. After ligation of the *Eco*RI-digested samples, the ligated DNA was further digested with *Mlu*I, which cuts the pX region of the HTLV-I genome and prevents amplification of the viral genome. Inverse long PCR was performed using Tks Gflex DNA Polymerase (Takara Bio). For the *Pst*I-treated group, the forward primer was 5'-CAGCCCATTCTATAGCACTCTCCAGGAGAG-3' and the reverse primer was 5'-CAGTCTCCAAACACGTAGACTGGG-TATCCG-3'. For the *Eco*RI-treated template, the forward primer was 5'-TGCCTGACCCTGCTTGCTCAACTCTACG-TCTTTG-3' and the reverse primer was 5'-AGTCTGGGCC-CTGACCTTTTCAGACTTCTGTTC-3'. Processed genomic DNA (50 ng) was used as a template. The reaction mixture was subjected to 35 cycles of denaturation (94°C, 30 seconds) and annealing plus extension (68°C, 8 minutes). Following PCR, the products were subjected to electrophoresis on 0.8% agarose gels. Fourteen patient samples were analyzed. For samples from which a sufficient amount of DNA was extracted, PCR was generally performed in duplicate.

Gene expression microarray analysis of each subpopulation in the CADM1 versus CD7 plot

Total RNA was extracted from each subpopulation in the CADM1 versus CD7 plot using TRIzol (Invitrogen) according to the manufacturer's protocol. Details of the clinical samples used for microarray analyses are shown in Supplementary Table S1. Treatment with DNase I (Takara Bio) was conducted to eliminate genomic DNA contamination. The quality of the extracted RNA was assessed using a BioAnalyzer 2000 system (Agilent Technologies). The RNA was then Cy3-labeled using a Low Input Quick Amp Labeling Kit (Agilent Technologies). Labeled cRNA samples were hybridized to 44K Whole Human Genome Oligonucleotide Microarrays (Agilent Technologies) at 65°C for 17 hours. After hybridization, the microarrays were washed and scanned with a Scanner C (Agilent Technologies). Signal intensities were evaluated by Feature Extraction 10.7 software and then analyzed using Gene Spring 12.0 software (Agilent Technologies). Unsupervised two-dimensional hierarchical clustering analysis (Pearson correlation) was performed on 10,278 genes selected by one-way ANOVA ($P < 0.05$). The dataset for these DNA microarrays has been deposited in Gene Expression Omnibus (accession number GSE55851).

Expression analysis of miR-31 and *Helios* transcript variants of each subpopulation in the CADM1 versus CD7 plot

The expression levels of the microRNA miR-31 were quantified using a TaqMan-based MicroRNA Assay (Applied Biosystems), as described previously (31), and normalized to RNU48 expression level. *Helios* mRNA transcript variants were examined using reverse transcription

PCR (RT-PCR) with Platinum Taq DNA Polymerase High Fidelity (Invitrogen), as described previously (32). To detect and distinguish alternative splicing variants, PCR analyses were performed with sense and antisense primer sets specific for the first and final exons of the Helios gene. The PCR products were then sequenced to determine the exact type of transcript variant. A mixture of Hel-1, Hel-2, Hel-5, and Hel-6 cDNA fragments was used as a "Helios standard" in the electrophoresis of RT-PCR samples.

Results

CADM1 expression based on the CD3 versus CD7 plot in CD4⁺ cells in primary HTLV-I-infected blood samples

The clinical profiles of the 32 cases analyzed are shown in Supplementary Table S1. We first examined CADM1 expression in each subpopulation (H, I, and L) of the CD3 versus CD7 plot. Representative data (for a case of smoldering ATL) are shown in Fig. 1A. The results demonstrate that

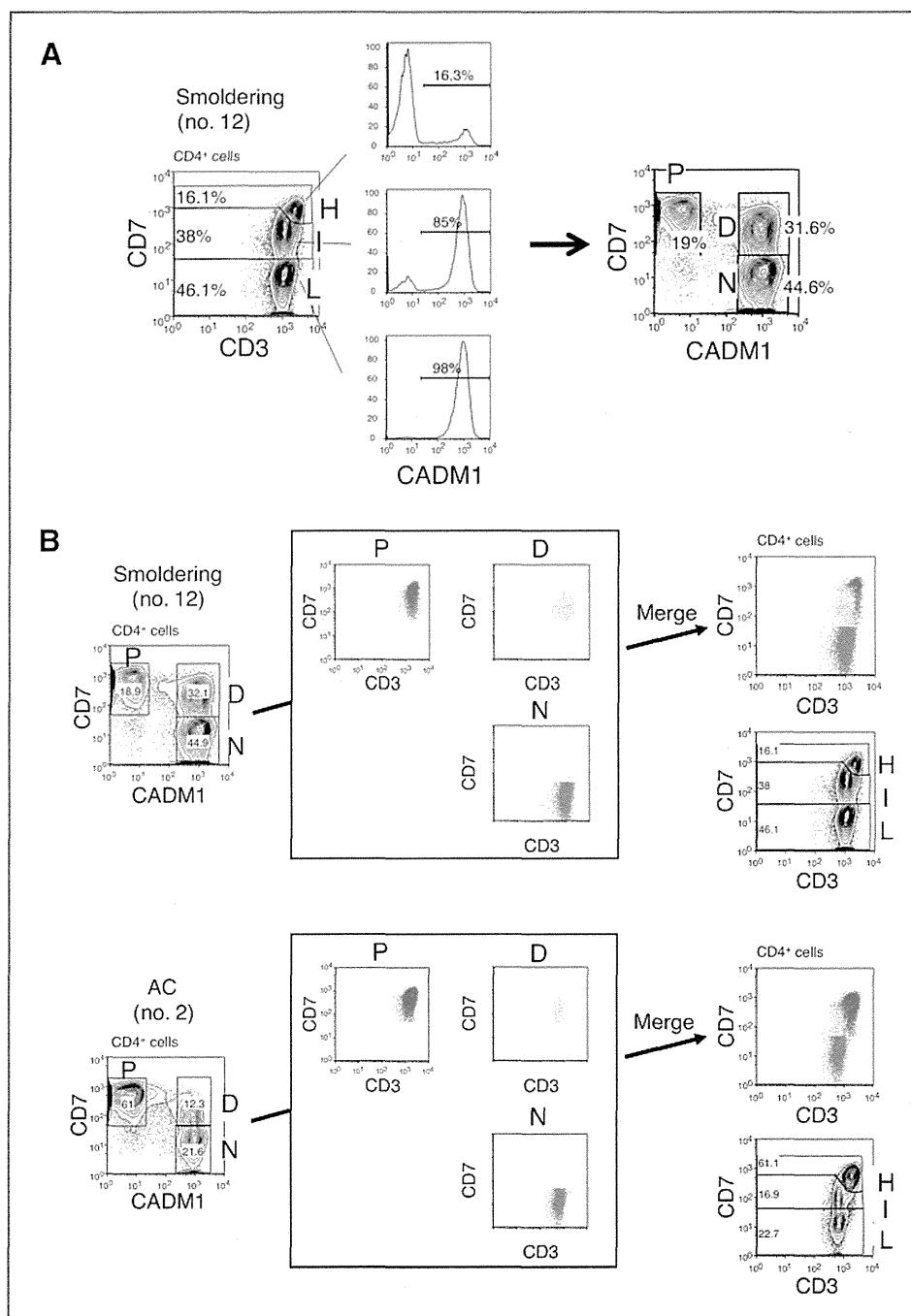


Figure 1. CADM1 versus CD7 plot for CD4⁺ cells from HTLV-I-infected blood samples analyzed by flow cytometry. **A**, representative flow-cytometric analysis of a patient with smoldering-type ATL. Three subpopulations (H, I, and L) were observed in the CD3 versus CD7 plot for CD4⁺ cells (left). Expression of CADM1 in each subpopulation is shown (middle). The right-hand panel shows how the CADM1 versus CD7 plot for CD4⁺ cells was constructed. **B**, the P, D, and N subpopulations in the CADM1 versus CD7 plot correspond to the H, I, and L subpopulations in the CD3 versus CD7 plot. Blue, yellow, and red dots, respectively, indicate the P, D, and N subpopulations in the CADM1 versus CD7 plot, and are redrawn in the CD3 versus CD7 plot. Two representative cases are shown. In the upper case, the P and D subpopulations in the CADM1 versus CD7 plot are partly intermingled in the CD3 versus CD7 plot. Unlike the CD3 versus CD7 plot, the CADM1 versus CD7 plot clearly distinguishes three subpopulations.

CADM1 was expressed almost exclusively in the I and L subpopulations. Drawing a CADM1 versus CD7 plot for CD4⁺ cells revealed three distinct subpopulations (P, CADM1^{neg}CD7^{pos}; D, CADM1^{pos}CD7^{dim}; and N, CADM1^{pos}CD7^{neg}). As shown in Fig. 1B, the P, D, and N subpopulations corresponded to the H, I, and L subpopulations in the CD3 versus CD7 plot. In the previous CD3 versus CD7 plot, the lower case (AC no. 2) showed three distinct subpopulations. However, in the upper case (smoldering no. 12), the H and I subpopulations substantially intermingled with each other and were not clearly separated. In contrast, the CADM1 versus CD7 plot clearly revealed three distinct subpopulations in both cases.

HTLV-I-infected cells are highly enriched in CADM1⁺ subpopulations

On the basis of previous reports (25, 27), we expected HTLV-I-infected cells to be enriched in the CADM1⁺ subpopulations in our analysis. Figure 2A shows the PVL measurements of the three subpopulations in the CADM1 versus CD7 plot for three representative cases. HTLV-I-infected cells were highly enriched in the CADM1⁺ subpopulations (D and N). The PVL data indicate that most of the cells in the D and N subpopulations were HTLV-I infected. Figure 2B shows the results of semiquantitative PCR of the *HBZ* gene in representative cases. In the D and N subpopulations, the *HBZ* gene was amplified to the same degree as in the HTLV-I-positive cell line. To confirm these results, FISH was performed in one asymptomatic carrier. As shown in Supplementary Fig. S2, HTLV-I-infected cells were highly enriched in the D and N subpopulations, which supports the results of the PVL analysis and semiquantitative PCR of the *HBZ* gene. In the FISH analysis, percentages of HTLV-I-infected cells in D and N did not reach 100%. This may have been due to a technical issue. Because the cells subjected to FISH analysis were sorted by FACS, several fluorochrome-conjugated

antibodies may have remained on their surfaces, even after treatment with protease.

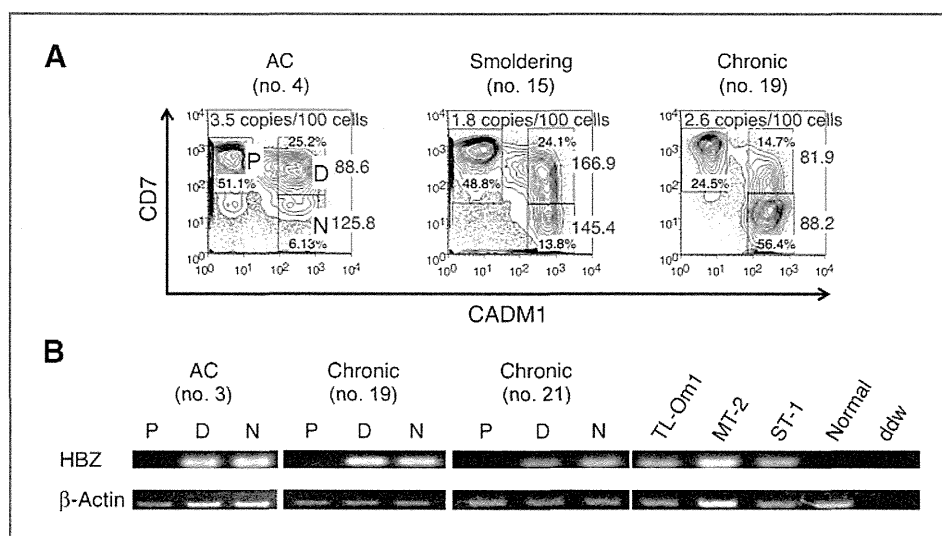
The CADM1 versus CD7 plot accurately reflects disease progression in HTLV-I infection

Compared with the CD3 versus CD7 plot, the CADM1 versus CD7 plot was revealed to be clear in its distinction of the three subpopulations and efficient in enrichment of HTLV-I-infected cells. On the basis of these findings, we analyzed clinical samples of asymptomatic carriers and three clinical subtypes of ATL: the smoldering, chronic, and acute subtypes. Data for representative cases, presented in Fig. 3A, suggest that the continual changes in the proportions of the three subpopulations are associated with disease progression. In the CADM1 versus CD7 plot, normal control samples showed a P-dominant pattern. With progression of the disease from the asymptomatic carrier state with a low PVL to that with a high PVL, and to indolent-type ATL, the D and N subpopulations increased gradually. As the disease further progressed to acute-type ATL, the N subpopulation showed remarkable expansion. Data for all analyzed samples are presented in Fig. 3B. The results suggest that the CADM1 versus CD7 plot of peripheral blood samples represents progression of the disease in HTLV-I carriers. Data for the normal control cases analyzed are shown in Supplementary Fig. S3. In all normal controls, the percentages of the D and N subpopulations were low. Supplementary Fig. S4 shows temporal data for a patient with chronic-type ATL who progressed from stable disease to a relatively progressive state and the concomitant change in the flow cytometry profile.

Clonality analysis of the three subpopulations in the CADM1 versus CD7 plot

To characterize the three subpopulations further, the clonal composition of each subpopulation was analyzed by inverse long PCR, which amplifies part of the provirus

Figure 2. HTLV-I-infected cells are highly enriched in the CADM1⁺ subpopulations. A, analysis of PVL in the three subpopulations. Three representative cases are shown. PVL data (copies/100 cells) are shown in red. Percentages of each subpopulation are shown in black. B, semiquantitative PCR of the *HBZ* gene in the three subpopulations in three representative cases. Normal, DNA from PBMCs from a normal control; ddw, deionized distilled water.



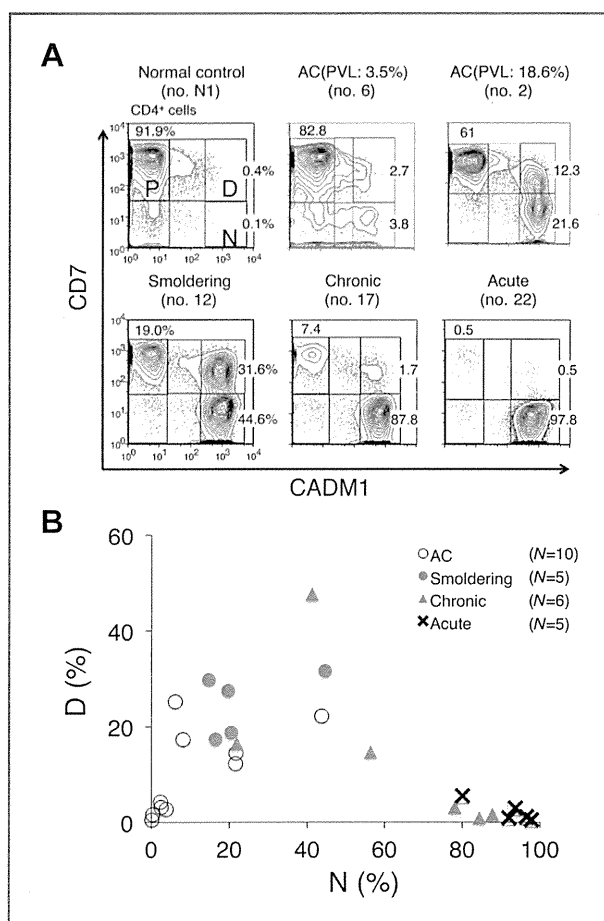


Figure 3. Proportion of each subpopulation in the CADM1 versus CD7 plots for asymptomatic HTLV-I carriers (asymptomatic carriers) and ATLs of various clinical subtypes. A, data of representative cases are shown. B, a two-dimensional plot of all analyzed samples showing the percentages of the D and N subpopulations.

long terminal repeat and the flanking genomic sequence of the integration sites. Cells in each subpopulation were sorted by FACS, and subjected to inverse long PCR analysis. Representative results for smoldering-, chronic-, and acute-type ATL samples are presented in Fig. 4A. Major clones, indicated by intense bands, were detected in the D and N subpopulations in each case. The major clones in the D and N subpopulations in each case were considered to be the same based on the sizes of the amplified bands, suggesting that clonal evolution is accompanied by downregulation of CD7 expression. Fig. 4B shows representative results for three cases of asymptomatic carrier. In all cases, weak bands in the P subpopulation were visible, indicating that this population contains only minor clones. In these asymptomatic carriers, the proportion of abnormal lymphocytes and PVL increases from left to right. The consistent increase in the D and N subpopulations, together with growth of major clones as shown in the inverse PCR analysis, were considered to reflect these clinical data.

Gene expression profiling of the three subpopulations in the CADM1 versus CD7 plot

To determine the molecular basis for the biologic differences among the three subpopulations in the CADM1 versus CD7 plot, we next characterized the gene-expression profiles of the subpopulations of the following clinical subgroups: asymptomatic carriers ($n = 2$), smoldering-type ATLs ($n = 2$), chronic-type ATL ($n = 1$), acute-type ATLs ($n = 3$), and normal controls ($n = 3$). The two asymptomatic carriers (nos. 5 and 9) had high PVLs (11.6 and 26.2%, respectively) and relatively high proportions of D and N subpopulations (Supplementary Table S1). Unsupervised hierarchical clustering analysis of the results revealed three clusters (A, B1, and B2) or two major clusters A and B, where A is composed solely of the samples of the acute-type N subpopulation and B is subdivided into two clusters (B1 and B2; Fig. 5A). The B2 cluster is composed of the P subpopulation of all clinical subtypes and of normal controls, whereas the B1 cluster is composed of the D and N subpopulations of

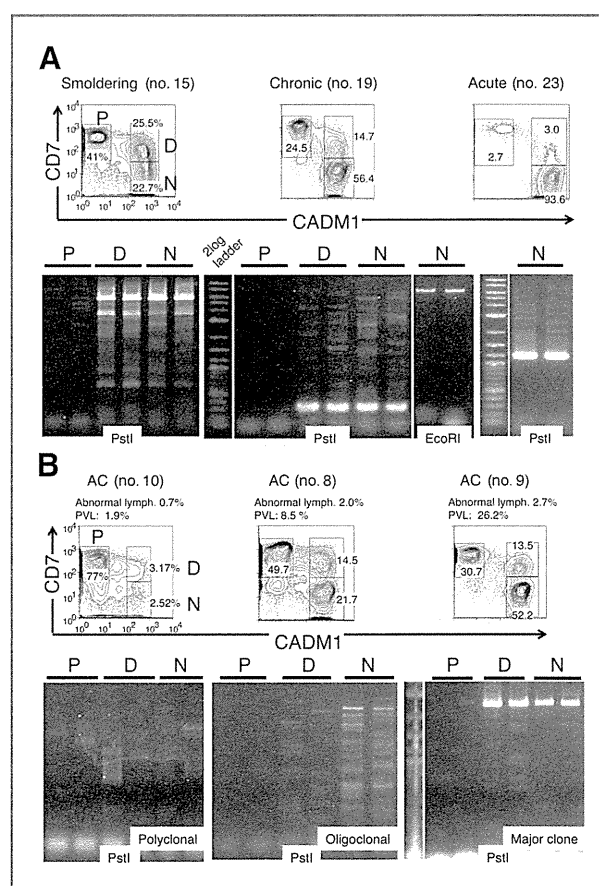


Figure 4. Clonality of subpopulations in the CADM1 versus CD7 plot analyzed by inverse long PCR. FACS-sorted cells (P, D, and N) were subjected to inverse long PCR. The black bar indicates duplicate data. Flow-cytometric profiles and clinical data are also presented. A, representative cases of smoldering-, chronic-, and acute-type ATL are shown. B, representative cases of asymptomatic carriers are shown.

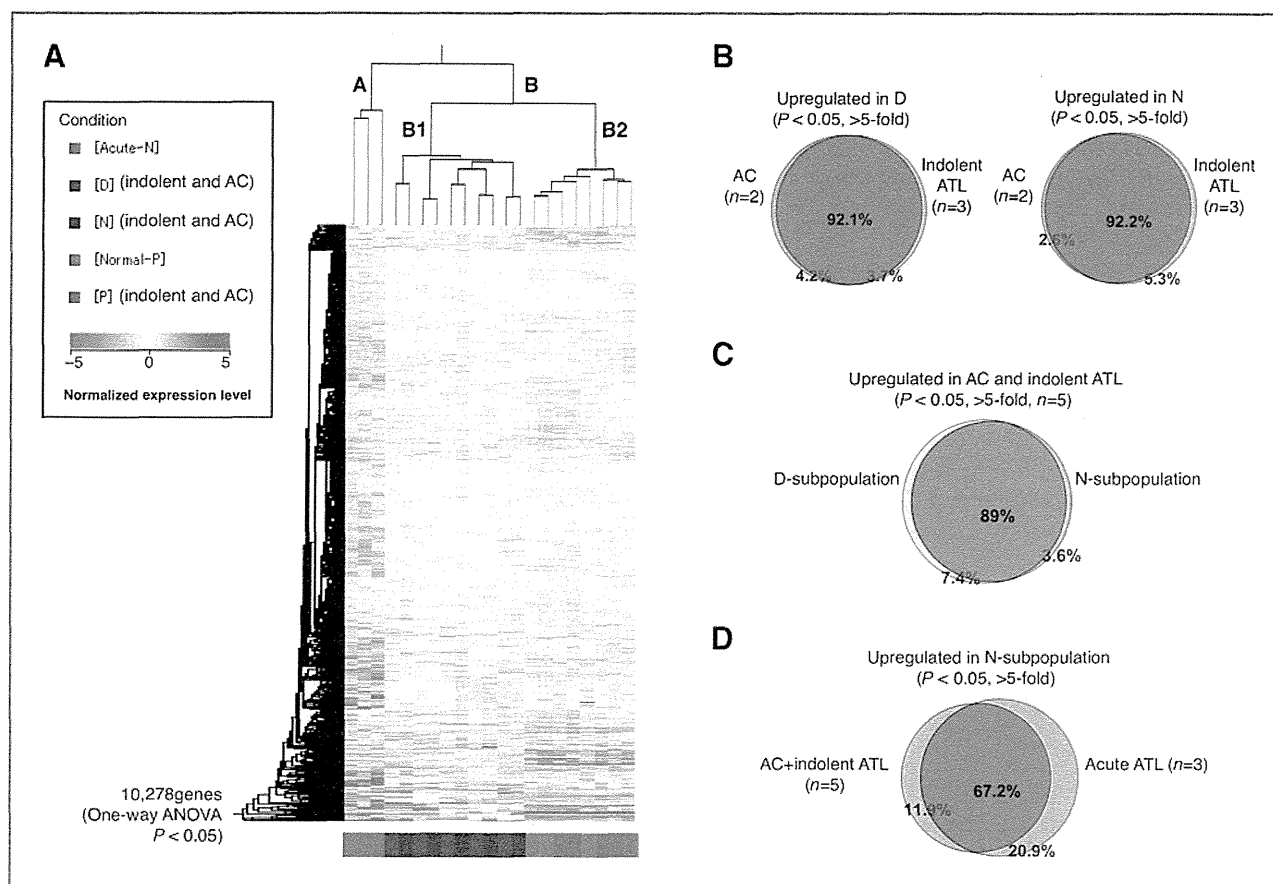


Figure 5. Comprehensive gene expression analysis of the three subpopulations in the CADM1 versus CD7 plot. A, we conducted an unsupervised hierarchical clustering analysis of 10,278 genes whose expression levels were significantly changed in the P subpopulation of normal controls ($n = 3$); P, D, and N subpopulations of asymptomatic carriers and indolent ATLs ($n = 5$); and N subpopulation of acute-ATLs ($n = 3$; one-way ANOVA, $P < 0.05$). The P and D subpopulations of acute ATLs and D and N subpopulations of normal controls could not be analyzed because of insufficient numbers of cells. Clustering resulted in three major clusters: (i) P subpopulations of normal controls (gray) and asymptomatic carriers/indolent ATLs (green); (ii) D and N subpopulations of asymptomatic carriers/indolent ATLs (blue and brown, respectively); and (iii) N subpopulations of acute ATLs (red). These results indicate that the P subpopulations of asymptomatic carriers/indolent ATLs have characteristics similar to those of normal uninfected cells, whereas the D and N subpopulations of asymptomatic carriers/indolent ATLs have genetic lesions in common. The N subpopulations of acute ATLs are grouped in an independent cluster, meaning that these malignant cell populations have a significantly different gene expression profile, even compared with the N subpopulations of indolent ATLs. B, similarity between asymptomatic carriers and indolent ATLs. The Venn diagrams show that 92.1% and 92.2% of genes upregulated in the D and N subpopulations, respectively, compared with "Normal-P" ($P < 0.05$), were common to asymptomatic carriers ($n = 2$) and indolent ATLs ($n = 3$). C, similarity between the D and N subpopulations. The Venn diagram shows that 89% of genes upregulated in the D and N subpopulation, compared with Normal-P ($P < 0.05$), overlapped. D, comparison of the N subgroups between acute-ATLs ($n = 3$) and asymptomatic carriers/indolent ATLs ($n = 5$). As shown in the Venn diagram, 67.2% of genes were upregulated ($P < 0.05$) in the N subpopulations of both acute ATLs and asymptomatic carrier/indolent ATLs. However, a significant number of genes (20.9%) were upregulated only in the N subpopulation of acute ATLs.

asymptomatic carriers and indolent ATLs (smoldering- and chronic-type).

Figure 5B shows a Venn diagram of the upregulated genes in the D subpopulation (left) or the N subpopulation (right) common to asymptomatic carriers ($n = 2$) and indolent ATLs ($n = 3$). These diagrams demonstrate that the changes in the gene expression profiles of the D and N subpopulations of asymptomatic carriers were similar to those of indolent ATLs. Furthermore, the gene expression profiles of the D and N subpopulations of asymptomatic carriers and indolent ATLs were similar (Fig. 5C). In contrast, the upregulated genes showed distinct differences between the N subpopulation of

acute-type ATL and that of indolent ATLs and asymptomatic carriers, although approximately 70% were common to both (Fig. 5D).

Expression of a tumor suppressor microRNA and splicing abnormalities of Ikaros family genes in the three subpopulations

To determine whether the novel subpopulations identified had other properties in common with ATL cells, we examined miR-31 levels and *Helios* mRNA patterns in sorted subpopulations (31, 32). Expression of miR-31 decreased drastically in the D subpopulation derived from indolent ATLs and asymptomatic carriers, and was

even lower in the N subpopulation derived from asymptomatic carriers and indolent/acute ATLs (Fig. 6A). In addition, examination of *Helios* mRNA transcript variants revealed that expression levels of *Hel-2*, which lacks part of exon 3, were upregulated in the D and N subpopulations of asymptomatic carriers and indolent ATLs, and it was dominantly expressed in the N subpopulation of acute ATLs (Fig. 6B).

Supplementary Fig. S5 presents a summary of this study. The representative flow-cytometric profile shows how the CADM1 versus CD7 plot reflects disease progression in HTLV-I infection. The plot together with the gene expression profiles clearly distinguished the subpopulations of distinct oncogenic stages. The groups classified according to gene expression profile are shown as blue, yellow, and red and are superimposed on the CADM1 versus CD7 plot. Collectively, our data suggest that CADM1 expression and stepwise downregulation of CD7 were closely associated

with clonal expansion of HTLV-I-infected cells in ATL progression.

Discussion

We showed that the CADM1 versus CD7 plot is capable of discriminating clonally expanding HTLV-I-infected cells in indolent ATLs and even in asymptomatic carriers, as well as in acute-type ATLs. Our analysis demonstrated efficient enrichment of HTLV-I-infected cells in the CADM⁺ subpopulations (D and N in the CADM1 vs. CD7 plot), based on the results of real-time PCR (PVL analysis), semiquantitative PCR analysis of the *HBZ* gene, and FISH analysis (Fig. 2 and Supplementary Fig. S2). Furthermore, the CADM1 versus CD7 plot was shown to discriminate the three subpopulations more clearly than the CD3 versus CD7-plot (Fig. 1). Clonality analysis of ATLs and asymptomatic carriers (Fig. 4A and B) revealed that CADM⁺ subpopulations (D and N) contained

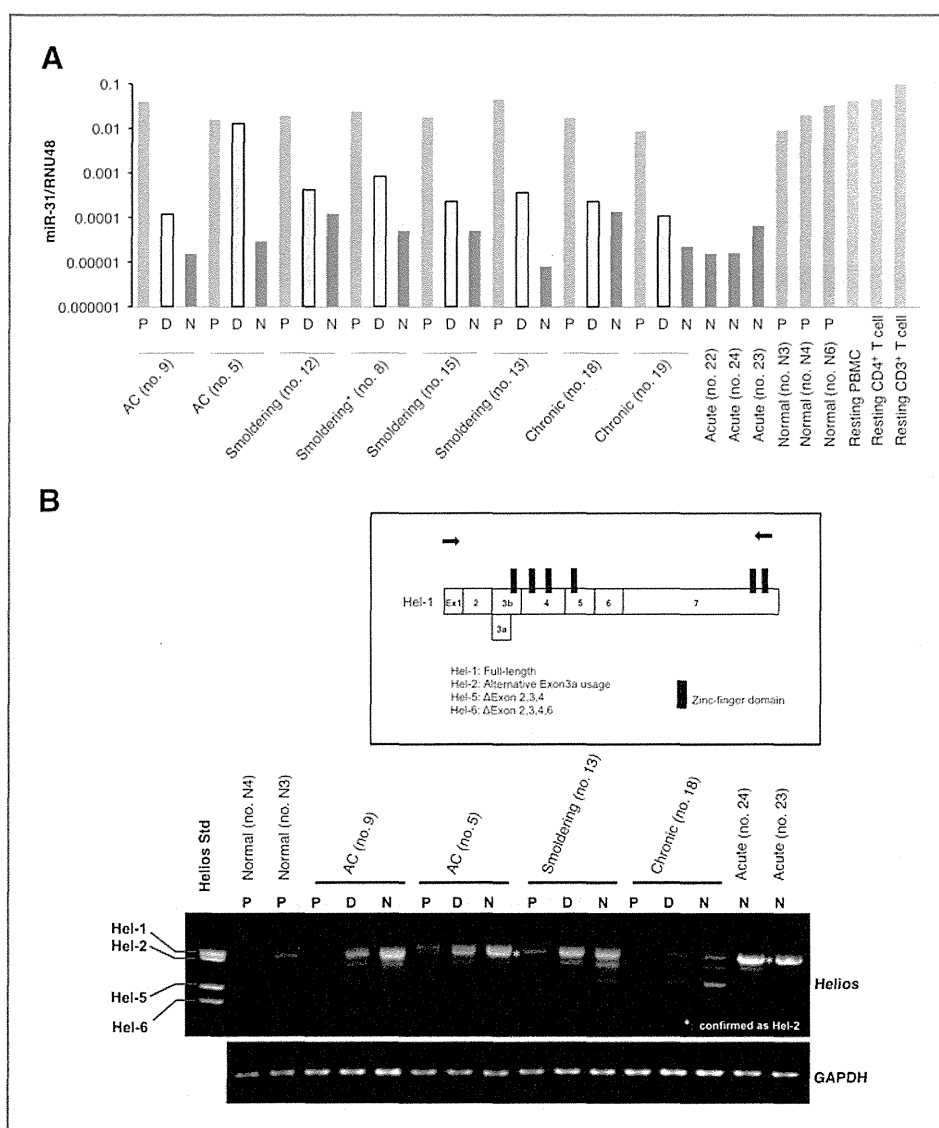


Figure 6. Gene expression pattern in the CADM1/CD7 subpopulation. A, miR-31 expression levels quantified by TaqMan-based real-time PCR. Total RNAs derived from each subpopulation were isolated and analyzed by RT-real-time PCR. RNU48 levels were also measured as an internal normalizer.

*Smoldering (no. 8), this patient was considered to be at the asymptomatic carrier/smoldering borderline, because the proportion of abnormal lymphocytes fluctuated around 5%. On the day of sampling, the patient's hemogram showed 6.5% abnormal lymphocytes. B, expression analysis of *Helios* transcript variants in the subpopulations of normal controls ($n = 2$), asymptomatic carriers ($n = 2$), and ATLs (smoldering-type ATL, $n = 1$; chronic-type ATL, $n = 1$; acute-type ATL, $n = 2$).

Comparisons of transcript variants among the P, D, and N subpopulations were performed by RT-PCR using primer sets specific for full-length *Helios* cDNA (top). The primer locations for *Helios* PCR are indicated by arrows in the schematic representation of *Hel-1*. The amplified cDNA (asterisk) was confirmed to be the *Hel-2* variant. The *Helios* standard (left lane), a mixture of cDNA fragments of *Hel-1*, *Hel-2*, *Hel-5*, and *Hel-6*, was used as a size indicator for each transcript variant. The glyceraldehyde-3-phosphate dehydrogenase (*gapdh*) mRNA was analyzed as an internal control (bottom).

clonally expanded HTLV-I-infected cells, whereas cells in the P subpopulation (CADM1⁻) did not show clonal expansion in this analysis. Current molecular analyses of ATL cells have been limited to HTLV-I-infected cell lines and primary cells from acute/lymphoma type ATL, because in these cases, the predominant expanding clones are readily available with relatively high purity. However, the separation of clonally expanding ATL cells from indolent ATLs and asymptomatic carriers has not yet been achieved. The CADM1 versus CD7 plot from FACS allows efficient purification of such clones *in vitro*.

In an unsupervised clustering analysis of the gene expression data, the D and N subpopulations of asymptomatic carriers/indolent ATLs were grouped together, suggesting that the biologic characteristics of these subpopulations are similar (Fig. 5A and B) but distinct from the N subpopulation of acute-type ATLs (Fig. 5D). These results support the notion that in indolent ATLs and even in asymptomatic carriers, the D and N subpopulations are clonally expanding cells representing the intermediate oncogenic stage. Although the D and N subpopulations have similar gene expression profiles (Fig. 5C), there are potentially important differences distinguishing these subpopulations, according to the apparent decrease in the D subpopulation and increase in the N subpopulation that were observed as the disease progressed from indolent to acute-type ATL (Fig. 3). Detailed analysis of the genomic and epigenomic differences between these two subpopulations will provide us with information about the genomic and epigenomic lesions that are involved in disease progression. Another important finding is that the expression profiles of cells in the N subpopulation of indolent and acute-type ATLs showed significant differences, even though the majority of the genes were common to both groups (Fig. 5D). Characterization of the genes that show distinct expression patterns will reveal the molecular events that contribute to the progression from indolent to aggressive ATLs.

To address whether the emerging molecular hallmark of ATL was conserved in the novel subpopulations identified, we examined the miR-31 level and *Helios* mRNA pattern in sorted subpopulations (Fig. 6). Through integrative analyses of ATL cells, we recently showed that the expression of miR-31, which negatively regulates noncanonical NF- κ B signaling by targeting NIK, is genetically and epigenetically suppressed in ATL cells, leading to persistent NF- κ B activation, and is thus inversely correlated with the malignancy of the cells (31). The miR-31 levels in the P subpopulations in asymptomatic carriers and indolent ATLs were as high as those in normal P subpopulations, PBMCs, and resting T cells, whereas those in the D subpopulations decreased significantly and those in the N subpopulations were as low as in acute-type N subpopulations (Fig. 6A). Previously, we also identified ATL-specific aberrant splicing of *Helios* mRNA and demonstrated its functional involvement in ATL (32). As shown in Fig. 6B, the *Hel-2* type variant, which lacks part of exon 3 and thus lacks one of the four DNA-binding zinc-finger domains, accumulated in the D and N subpopulations of asymptomatic carriers and indolent ATLs, and

was dominantly expressed in the N subpopulation of acute-type ATLs. Collectively, the molecular abnormality of ATL cells became evident in the gradual progression from P to D to N, even in asymptomatic carriers, strongly supporting the notion that the CADM1/CD7 expression pattern correlates with the multistep oncogenesis of ATL.

One of the more remarkable findings in the expression profile analysis was that the D and N subpopulations of asymptomatic carriers clustered within the same group as those of the indolent ATL cases (Fig. 5A and B). The asymptomatic carriers used in this analysis had high PVLs and relatively high proportions of the D and N subpopulations (Supplementary Table S1). In addition, mono- or oligoclonal expansion of the HTLV-I-infected cells was demonstrated in these cases. HTLV-I-infected cells in the D and N subpopulations of these asymptomatic carriers comprise clonally expanding cells that are potentially at the premalignant and intermediate stages according to their clonality, comprehensive gene expression profile, miR31 expression, and aberrant RNA splicing, all indicating that they can be categorized as asymptomatic carriers with high risk of developing into ATL, requiring careful follow-up (15, 30, 33, 34). Our flow-cytometric analysis of PBMCs from asymptomatic carriers using the CADM1 versus CD7 plot may provide a powerful tool for identifying high-risk asymptomatic carriers. Certain indolent ATL cases are difficult to distinguish from asymptomatic carriers, according to Shimoyama's criteria based on the morphologic characteristics determined by microscopic examination. Characterization of peripheral blood T cells by the CADM1 versus CD7 plot may provide useful information for clinical diagnosis.

According to Masuda and colleagues, manipulation of *CADM1* gene expression in leukemic cell lines suggested that *CADM1* expression confers upon ATL cells tissue invasiveness and a growth advantage (35). The mechanism by which HTLV-I infection regulates *CADM1* expression and the significance of *CADM1* expression in ATL oncogenesis will require clarification by future studies.

Finally, as summarized in Supplementary Fig. S5, we demonstrated that (1) HTLV-I-infected and clonally expanded cells are efficiently enriched in *CADM1*⁺ subpopulations; (2) the proportions of the three subpopulations in the *CADM1* versus CD7 plot, discriminated by *CADM1* expression and stepwise downregulation of CD7, accurately reflect the disease stage in HTLV-I infection; and (3) the *CADM1*⁺CD7^{dim/neg} subpopulations are at the intermediate stage of ATL progression and can be identified even in asymptomatic carriers. These findings will help to elucidate the molecular events involved in multistep oncogenesis of ATL.

Disclosure of Potential Conflicts of Interest

No potential conflicts of interest were disclosed.

Authors' Contributions

Conception and design: S. Kobayashi, T. Watanabe, K. Uchimar

Development of methodology: T. Ishigaki, T. Yamochi, N. Watanabe

Acquisition of data (provided animals, acquired and managed patients, provided facilities, etc.): S. Kobayashi, E. Watanabe, K. Yuji, N. Oyaizu, S. Asanuma, A. Tojo

Analysis and interpretation of data (e.g., statistical analysis, biostatistics, computational analysis): S. Kobayashi, K. Nakano, T. Ishigaki, N. Oyaizu, M. Yamagishi, T. Watanabe

Writing, review, and/or revision of the manuscript: S. Kobayashi, K. Nakano, A. Tojo, T. Watanabe, K. Uchimaru

Administrative, technical, or material support (i.e., reporting or organizing data, constructing databases): T. Ishigaki, N. Ohno, N. Watanabe
Study supervision: A. Tojo, T. Watanabe, K. Uchimaru

Acknowledgments

The authors thank Drs. Kazunari Yamaguchi (National Institute of Infectious Diseases, Tokyo, Japan) and Yoshinori Murakami (the University of Tokyo) for their constructive comments; Yuji Zaiki (Clinical Laboratory, Research Hospital, Institute of Medical Science, the University of Tokyo) for his excellent technical advice; Keisuke Takahashi, Sanae Suzuki, and mem-

bers of our laboratory for assistance; and the hospital staff, which has made a commitment to providing high-quality care to all patients. The English in this document has been checked by at least two professional editors, both native speakers of English.

Grant Support

This work was supported by grants-in-aid for scientific research awarded to K. Uchimaru (no. 22591028) and T. Watanabe (no. 23390250) by the Ministry of Education, Culture, Sports, Science and Technology of Japan.

The costs of publication of this article were defrayed in part by the payment of page charges. This article must therefore be hereby marked *advertisement* in accordance with 18 U.S.C. Section 1734 solely to indicate this fact.

Received November 19, 2013; revised March 19, 2014; accepted March 26, 2014; published OnlineFirst April 11, 2014.

References

- Yoshida M, Miyoshi I, Hinuma Y. Isolation and characterization of retrovirus from cell lines of human adult T-cell leukemia and its implication in the disease. *Proc Natl Acad Sci U S A* 1982;79:2031-5.
- Osame M, Usuku K, Izumo S, Ijichi N, Amitani H, Igata A, et al. HTLV-I associated myelopathy, a new clinical entity. *Lancet* 1986;1:1031-2.
- Mochizuki M, Watanabe T, Yamaguchi K, Takatsuki K, Yoshimura K, Shirao M, et al. HTLV-I uveitis: a distinct clinical entity caused by HTLV-I. *Jpn J Cancer Res* 1992;83:236-9.
- Yamaguchi K, Watanabe T. Human T lymphotropic virus type-I and adult T-cell leukemia in Japan. *Int J Hematol* 2002;76 Suppl 2:240-5.
- Murphy EL, Hanchard B, Figueroa JP, Gibbs WN, Lofters WS, Campbell M, et al. Modelling the risk of adult T-cell leukemia/lymphoma in persons infected with human T-lymphotropic virus type I. *Int J Cancer* 1989;43:250-3.
- Iwanaga M, Watanabe T, Yamaguchi K. Adult T-cell leukemia: a review of epidemiological evidence. *Front Microbiol* 2012;3:322.
- Okamoto T, Ohno Y, Tsugane S, Watanabe S, Shimoyama M, Tajima K, et al. Multi-step carcinogenesis model for adult T-cell leukemia. *Jpn J Cancer Res* 1989;80:191-5.
- Matsuoka M, Jeang KT. Human T-cell leukemia virus type 1 (HTLV-1) and leukemic transformation: viral infectivity, Tax, HBZ and therapy. *Oncogene* 2011;30:1379-89.
- Matsuoka M, Jeang KT. Human T-cell leukaemia virus type 1 (HTLV-1) infectivity and cellular transformation. *Nat Rev Cancer* 2007;7:270-80.
- Yoshida M. Molecular approach to human leukemia: isolation and characterization of the first human retrovirus HTLV-1 and its impact on tumorigenesis in adult T-cell leukemia. *Proc Jpn Acad Ser B Phys Biol Sci* 2010;86:117-30.
- Yamagishi M, Watanabe T. Molecular hallmarks of adult T cell leukemia. *Front Microbiol* 2012;3:334.
- Tsukasaki K, Hermine O, Bazarbachi A, Ratner L, Ramos JC, Harrington W Jr, et al. Definition, prognostic factors, treatment, and response criteria of adult T-cell leukemia-lymphoma: a proposal from an international consensus meeting. *J Clin Oncol* 2009;27:453-9.
- Ishida T, Joh T, Ujike N, Yamamoto K, Utsunomiya A, Yoshida S, et al. Defucosylated anti-CCR4 monoclonal antibody (KW-0761) for relapsed adult T-cell leukemia-lymphoma: a multicenter phase II study. *J Clin Oncol* 2012;30:837-42.
- Tian Y, Kobayashi S, Ohno N, Isobe M, Tsuda M, Zaiki Y, et al. Leukemic T cells are specifically enriched in a unique CD3(dim) CD7 (low) subpopulation of CD4(+) T cells in acute-type adult T-cell leukemia. *Cancer Sci* 2011;102:569-77.
- Kobayashi S, Tian Y, Ohno N, Yuji K, Ishigaki T, Isobe M, et al. The CD3 versus CD7 Plot in Multicolor Flow Cytometry Reflects Progression of Disease Stage in Patients Infected with HTLV-I. *PLoS One* 2013;8:e53728.
- Reinhold U, Abken H. CD4+ CD7- T cells: a separate subpopulation of memory T cells? *J Clin Immunol* 1997;17:265-71.
- Reinhold U, Abken H, Kukel S, Moll M, Muller R, Oltmann I, et al. CD7- T cells represent a subset of normal human blood lymphocytes. *J Immunol* 1993;150:2081-9.
- Leblond V, Othman TB, Blanc C, Theodorou I, Choquet S, Sutton L, et al. Expansion of CD4+CD7- T cells, a memory subset with preferential interleukin-4 production, after bone marrow transplantation. *Transplantation* 1997;64:1453-9.
- Aandahl EM, Quigley MF, Moretto WJ, Moll M, Gonzalez VD, Sonnerborg A, et al. Expansion of CD7(low) and CD7(negative) CD8 T-cell effector subsets in HIV-1 infection: correlation with antigenic load and reversion by antiretroviral treatment. *Blood* 2004;104:3672-8.
- Autran B, Legac E, Blanc C, Debre P. A Th0/Th2-like function of CD4+CD7- T helper cells from normal donors and HIV-infected patients. *J Immunol* 1995;154:1408-17.
- Legac E, Autran B, Merle-Beral H, Katlama C, Debre P. CD4+CD7- CD57+ T cells: a new T-lymphocyte subset expanded during human immunodeficiency virus infection. *Blood* 1992;79:1746-53.
- Schmidt D, Goronzy JJ, Weyand CM. CD4+ CD7- CD28- T cells are expanded in rheumatoid arthritis and are characterized by autoreactivity. *J Clin Invest* 1996;97:2027-37.
- Willard-Gallo KE, Van de Keere F, Kettmann R. A specific defect in CD3 gamma-chain gene transcription results in loss of T-cell receptor/CD3 expression late after human immunodeficiency virus infection of a CD4+ T-cell line. *Proc Natl Acad Sci U S A* 1990;87:6713-7.
- Sasaki H, Nishikata I, Shiraga T, Akamatsu E, Fukami T, Hidaka T, et al. Overexpression of a cell adhesion molecule, TSLC1, as a possible molecular marker for acute-type adult T-cell leukemia. *Blood* 2005;105:1204-13.
- Nakahata S, Morishita K. CADM1/TSLC1 is a novel cell surface marker for adult T-cell leukemia/lymphoma. *J Clin Exp Hematop* 2012;52:17-22.
- Kuramochi M, Fukuhara H, Nobukuni T, Kanbe T, Maruyama T, Ghosh HP, et al. TSLC1 is a tumor-suppressor gene in human non-small-cell lung cancer. *Nat Genet* 2001;27:427-30.
- Nakahata S, Saito Y, Marutsuka K, Hidaka T, Maeda K, Hatakeyama K, et al. Clinical significance of CADM1/TSLC1/IgSF4 expression in adult T-cell leukemia/lymphoma. *Leukemia* 2012;26:1238-46.
- Sugamura K, Fujii M, Kannagi M, Sakitani M, Takeuchi M, Hinuma Y. Cell surface phenotypes and expression of viral antigens of various human cell lines carrying human T-cell leukemia virus. *Int J Cancer* 1984;34:221-8.
- Shimoyama M. Diagnostic criteria and classification of clinical subtypes of adult T-cell leukaemia-lymphoma. A report from the Lymphoma Study Group (1984-87). *Br J Haematol* 1991;79:428-37.
- Iwanaga M, Watanabe T, Utsunomiya A, Okayama A, Uchimaru K, Koh KR, et al. Human T-cell leukemia virus type I (HTLV-1) proviral load and

- disease progression in asymptomatic HTLV-1 carriers: a nationwide prospective study in Japan. *Blood* 2010;116:1211-9.
31. Yamagishi M, Nakano K, Miyake A, Yamoichi T, Kagami Y, Tsutsumi A, et al. Polycomb-mediated loss of miR-31 activates NIK-dependent NF- κ B pathway in adult T cell leukemia and other cancers. *Cancer Cell* 2012;21:121-35.
 32. Asanuma S, Yamagishi M, Kawanami K, Nakano K, Sato-Otsubo A, Muto S, et al. Adult T-cell leukemia cells are characterized by abnormalities of Helios expression that promote T-cell growth. *Cancer Sci* 2013;104:1097-106.
 33. Yamaguchi K, Kiyokawa T, Nakada K, Yul LS, Asou N, Ishii T, et al. Polyclonal integration of HTLV-I proviral DNA in lymphocytes from HTLV-I seropositive individuals: an intermediate state between the healthy carrier state and smoldering ATL. *Br J Haematol* 1988;68:169-74.
 34. Kamihira S, Iwanaga M, Doi Y, Sasaki D, Mori S, Tsurda K, et al. Heterogeneity in clonal nature in the smoldering subtype of adult T-cell leukemia: continuity from carrier status to smoldering ATL. *Int J Hematol* 2012;95:399-408.
 35. Masuda M, Maruyama T, Ohta T, Ito A, Hayashi T, Tsukasaki K, et al. CADM1 interacts with Tiam1 and promotes invasive phenotype of human T-cell leukemia virus type I-transformed cells and adult T-cell leukemia cells. *J Biol Chem* 2010;285:15511-22.

Clinical Cancer Research

CADM1 Expression and Stepwise Downregulation of CD7 Are Closely Associated with Clonal Expansion of HTLV-I–Infected Cells in Adult T-cell Leukemia/Lymphoma

Seiichiro Kobayashi, Kazumi Nakano, Eri Watanabe, et al.

Clin Cancer Res 2014;20:2851-2861. Published OnlineFirst April 11, 2014.

Updated version Access the most recent version of this article at:
[doi:10.1158/1078-0432.CCR-13-3169](https://doi.org/10.1158/1078-0432.CCR-13-3169)

Supplementary Material Access the most recent supplemental material at:
<http://clincancerres.aacrjournals.org/content/suppl/2014/04/16/1078-0432.CCR-13-3169.DC1.html>

Cited Articles This article cites by 35 articles, 11 of which you can access for free at:
<http://clincancerres.aacrjournals.org/content/20/11/2851.full.html#ref-list-1>

Citing articles This article has been cited by 1 HighWire-hosted articles. Access the articles at:
<http://clincancerres.aacrjournals.org/content/20/11/2851.full.html#related-urls>

E-mail alerts Sign up to receive free email-alerts related to this article or journal.

Reprints and Subscriptions To order reprints of this article or to subscribe to the journal, contact the AACR Publications Department at pubs@aacr.org.

Permissions To request permission to re-use all or part of this article, contact the AACR Publications Department at permissions@aacr.org.

Advanced human T-cell leukemia virus type 1 carriers and early-stage indolent adult T-cell leukemia-lymphoma are indistinguishable based on CADM1 positivity in flow cytometry

Seiichiro Kobayashi,¹ Eri Watanabe,² Tomohiro Ishigaki,² Nobuhiro Ohno,³ Koichiro Yuji,⁴ Kazumi Nakano,⁵ Tadanori Yamochi,⁵ Nobukazu Watanabe,² Arinobu Tojo,^{1,3} Toshiki Watanabe⁵ and Kaoru Uchimaru³

¹Division of Molecular Therapy, Institute of Medical Science, The University of Tokyo, Tokyo; ²Laboratory of Diagnostic Medicine, Institute of Medical Science, The University of Tokyo, Tokyo; ³Department of Hematology/Oncology, Research Hospital, Institute of Medical Science, The University of Tokyo, Tokyo; ⁴Project Division of International Advanced Medical Research, Institute of Medical Science, The University of Tokyo, Tokyo; ⁵Graduate School of Frontier Sciences, The University of Tokyo, Tokyo, Japan

Key words

Adult T-cell leukemia-lymphoma, CADM1 protein, CD7 antigen, flow cytometry, HTLV-1

Correspondence

Kaoru Uchimaru, 4-6-1 Shirokanedai, Minato-ku, Tokyo 108-8639, Japan.
Tel: 81-3-5449-5542; Fax: 81-3-5449-5429;
E-mail: uchimaru@ims.u-tokyo.ac.jp

Funding Information

Ministry of Education, Culture, Sports, Science and Technology of Japan (22591028, 23390250), Ministry of Health, Labor and Welfare of Japan (H26-sink-oujitsuyuoka-ippan-013).

Received December 15, 2014; Revised February 4, 2015;
Accepted February 12, 2015

Cancer Sci (2015)

doi: 10.1111/cas.12639

We previously reported that the cell adhesion molecule 1 (CADM1) versus CD7 plot in flow cytometry reflects disease progression in human T-cell leukemia virus type 1 (HTLV-1) infection. In CD4⁺ cells from peripheral blood, CADM1⁻CD7⁺ (P), CADM1⁺CD7^{dim} (D) and CADM1⁺CD7⁻ (N) subpopulations are observed. The D and N subpopulations increase as asymptomatic HTLV-1 carriers (AC) progress to indolent adult T-cell leukemia-lymphoma (ATL) and the N subpopulation then expands in aggressive ATL. In the present study we examined whether the analysis can estimate the risk of developing ATL in advanced AC. Peripheral blood samples from AC (N = 41) and indolent ATL patients (N = 19) were analyzed by flow cytometry using the CADM1 versus CD7 plot for CD4⁺ cells and inverse long PCR (clonality analysis) of FACS-sorted subpopulations. Almost all AC with a high HTLV-1 proviral load (>4 copies/100 cells) had a CADM1⁺ (D + N) frequency of >10%. AC with 25% < CADM1⁺ ≤ 50% contained expanded clones similar to smoldering-type ATL. In many patients in the 25% < CADM1⁺ ≤ 50% group, the proportion of abnormal lymphocytes was distributed around the 5% line, which divides AC and smoldering-type ATL in Shimoyama's classification. In conclusion, the CADM1 versus CD7 plot is useful for selection of putative high-risk AC. The characteristics of some AC and smoldering ATL are said to be similar; however, long-term follow up is required and the clinical outcome (e.g. rate of transformation) of these cases should be used to determine whether to include them in the same clinical category.

Human T-cell leukemia virus type 1 (HTLV-1) is a human retrovirus that causes HTLV-1-associated diseases such as adult T-cell leukemia-lymphoma (ATL, a neoplastic disease of CD4⁺ T cells), HTLV-1-associated myelopathy/tropical spastic paraparesis (HAM, a chronic inflammatory disease of the central nervous system) and HTLV-1 uveitis (HU, a subacute inflammatory disease of the uvea).⁽¹⁻³⁾ A recent report estimated that 5–10 million people are HTLV-1-infected worldwide.⁽⁴⁾ In Japan, the estimated lifetime risk of developing ATL in HTLV-1 asymptomatic carriers (AC) is 6–7% for males and 2–3% for females.⁽⁵⁻⁷⁾

We recently developed a flow cytometry-based method that enables HTLV-1-infected and clonally expanding cells to be purified.⁽⁸⁻¹⁰⁾ In the cell adhesion molecule 1 (CADM1) versus CD7 plot for CD4⁺ cells in peripheral blood mononuclear cells (PBMC) from HTLV-1-infected patients, three subpopulations (P, CADM1⁻CD7⁺; D, CADM1⁺CD7^{dim}; and N, CADM1⁺CD7⁻) are consistently observed.⁽¹⁰⁾ HTLV-1-infected cell clones are enriched in the CADM1⁺ subpopulations (D and

N). In the early stage of ATL development (from AC to indolent ATL), the D and N subpopulations increase concomitantly with clonal growth of these subpopulations. In the late stage (from indolent ATL to aggressive ATL), the N subpopulation expands, indicating loss of CD7 in the CADM1⁺ subpopulations. Therefore, the CADM1 versus CD7 profile enables objective evaluation of HTLV-1 disease progression regardless of the disease stage in HTLV-1 infection.

Factors associated with development of ATL have been reported to include HTLV-1 infection through breastfeeding, advanced age and family history of ATL.^(7,11) A recent epidemiological study in Japan revealed that AC with a high proviral load (PVL, more than four copies per 100 PBMC) are at high risk of developing ATL.⁽¹²⁾ Other definitive risk factors for the development of ATL have not been determined.

In this study we propose that our flow cytometry (CADM1 versus CD7 plot) will help to identify high-risk AC. The flow cytometric profiles of AC varied widely, with some AC having increased CADM1⁺ subpopulations to the same degree

as indolent ATL. These AC were indistinct from early-stage indolent ATL based on the CADM1 versus CD7 profile, clonality analysis and clinical data (PVL and percentage of abnormal lymphocytes). Our flow cytometric analysis revealed that some AC and smoldering ATL have similar characteristics, indicating the need for careful clinical follow up of these cases and that flow cytometry can be used to identify putative high-risk AC.

Materials and Methods

Cell lines and patient samples. TL-Om1, an HTLV-1-infected cell line, was provided by Dr Sugamura (Tohoku University, Sendai, Japan). Peripheral blood samples were collected from inpatients and outpatients at our hospital from June 2011 to September 2014, as described in our previous reports.^(8–10) As shown in Table 1, 60 cases were analyzed (41 AC; 9 cases of smoldering-type ATL; 10 cases of chronic-type ATL). All patients with ATL were categorized into clinical subtypes according to Shimoyama's criteria.^(13,14) Patients with various complications, such as autoimmune disorders and systemic infections, were excluded. The present study was approved by the Institutional Review Board of our institute (University of Tokyo). Written informed consent was obtained from all patients.

Flow cytometry and cell sorting. Peripheral blood mononuclear cells were isolated from whole blood by density gradient centrifugation, as described previously.⁽⁸⁾ An unlabeled CADM1 antibody (clone 3E1) and an isotype control chicken IgY antibody were purchased from MBL (Nagoya, Japan). These were biotinylated (by primary amine biotinylation) using biotin *N*-hydroxysuccinimide ester (Sigma Aldrich, St. Louis, MO, USA). A Pacific Orange-conjugated anti-CD14 antibody was purchased from Life Technologies (Carlsbad, CA, USA). All other antibodies were obtained from BioLegend (San Diego, CA, USA). Cells were stained using a combination of biotin-CADM1, allophycocyanin (APC)-CD7, APC-Cy7-CD3, Pacific Blue-CD4 and Pacific Orange-CD14. After washing, phycoerythrin (PE)-conjugated streptavidin was applied. Propidium iodide (PI [Sigma Aldrich]) was added to the samples to stain dead cells immediately before flow cytometry. A FACSAria instrument (BD Immunocytometry Systems, San Jose, CA, USA) was used for all multicolor flow cytometry and fluorescence-activated cell sorting (FACS). Data were analyzed using the FlowJo software (TreeStar, San Carlos, CA, USA). The gating procedure was as described previously.⁽¹⁰⁾ Briefly, PI⁺ cells and then CD14⁺ cells were gated out. Next, a CADM1 versus CD7 plot for CD4⁺ cells was constructed (Fig. 1a).

Quantification of human T-cell leukemia virus type 1 proviral load by real-time quantitative PCR. Proviral load in FACS-sorted PBMC was quantified by real-time quantitative PCR

(TaqMan method) using the ABI Prism 7000 sequence detection system (Applied Biosystems, Foster City, CA, USA), as described previously.^(8,12)

Inverse long PCR to assess the clonality of human T-cell leukemia virus type 1-infected cells. For clonality analysis, inverse long PCR was performed as described previously.⁽⁸⁾ First, 1 µg of genomic DNA extracted from FACS-sorted cells was digested with PstI at 37°C overnight. RNase A (Qiagen, Hilden, Germany) was added to remove residual RNA completely. DNA fragments were purified using a QIAEX2 gel extraction kit (Qiagen). The purified DNA was self-ligated with T4 DNA ligase (Takara Bio, Otsu, Japan) at 16°C overnight. Inverse long PCR was performed using Tks Gflex DNA Polymerase (Takara Bio). The forward primer was 5'-CAGCCATTCTATAGCACTCTCCAGGAGAG-3' and the reverse primer was 5'-CAGTCTCCAAACACGTAGACTGGGTATCCG-3'. Processed genomic DNA (50 ng) was used as the template. The reaction mixture was subjected to 35 cycles of denaturation (94°C, 30 s) and annealing plus extension (68°C, 8 min). The PCR products were subjected to electrophoresis on 0.8% agarose gels. For samples from which a sufficient amount of DNA was extracted, PCR was generally performed in duplicate.

Statistical analyses. Statistical comparisons were performed by Kruskal–Wallis non-parametric ANOVA and Dunn's procedure for pairwise comparisons using GraphPad Prism version 5.0a (GraphPad Software, San Diego, CA, USA). *P* < 0.05 was taken to indicate statistical significance.

Results

Asymptomatic carriers with high proviral load have increased CADM1⁺ subpopulations. Because high PVL (more than four copies per 100 PBMC) is one of the major risk factors for AC to develop ATL,⁽¹²⁾ we first analyzed the relationship between the CADM1 versus CD7 profile and PVL. A representative CADM1 versus CD7 profile is shown in Figure 1(a). As shown in Figure 1(b), almost all AC with high PVL had CADM1⁺ (D + N) subpopulations of >10% (24 of 25 cases). Conversely, AC with a CADM1⁺ population of ≤10% predominate in those with a PVL of fewer than four copies per 100 PBMC (15 of 16 cases). In this study, CADM1⁺ (%) indicates the proportion of CD4⁺ cells that were CADM1⁺ unless otherwise stated. PVL indicates the number of HTLV-1 copies/100 PBMC (HTLV-1-infected T cells generally contain a single integrated provirus).⁽¹⁵⁾ To compare both factors directly, the CADM1⁺ (%) for PBMC was calculated by taking the percentage of CD4⁺ cells and all lymphocytes into account. As shown in Figure S1, the CADM1⁺ (%) for PBMC was nearly equal to the PVL in AC.

Clonality analysis of CADM1⁺ subpopulations in asymptomatic carriers and indolent ATL. The three subpopulations (P, D and N) in the CADM1 versus CD7 plot were FACS-sorted and subjected to clonality analysis (by inverse long PCR).

Table 1. Clinical profile of HTLV-1 infected patients in the present study

Clinical subtype	Number of cases	Male	Female	Age (range)	WBC (per µL) (range)	Lymphocytes (%) (range)	Abnormal lymphocytes (%) (range)
HTLV-1 AC	41	14	27	52.8 (31–69)	5694 (3110–10360)	33.0 (17.5–44.5)	1.9 (0.0–4.7)
Smoldering	9	3	6	56.0 (43–72)	5561 (2620–7270)	29.9 (11.0–39.5)	9.3 (5.0–24.5)
Chronic	10	5	5	54.3 (43–67)	12345 (7780–25570)	31.6 (5.5–64.0)	32.1 (6.0–60.5)

Average of age, WBC, lymphocytes (%) and abnormal lymphocytes (%) are shown. Proportion of abnormal lymphocytes in the peripheral blood WBC were evaluated by morphological examination. AC, asymptomatic carrier; HTLV-1, human T-cell leukemia virus type 1; WBC, white blood cells (normal range, 3500–9100/µL).

Fig. 1. The cell adhesion molecule 1 (CADM1) versus CD7 profile in asymptomatic HTLV-1 carriers (AC) correlates with proviral load (PVL). (a) A representative CADM1 versus CD7 profile for CD4⁺ cells. P (CADM1⁻CD7⁺), D (CADM1⁺CD7^{dim}) and N (CADM1⁺CD7⁻) subpopulations were gated according to our previous report.⁽¹⁰⁾ (b) Almost all AC with PVL >4 copies/100 peripheral blood mononuclear cells (PBMC) had CADM1⁺ (D + N) values of more than 10% in the CADM1 versus CD7 plot, and almost all AC with PVL <4 copies/100 PBMC had CADM1⁺ values of <10%.

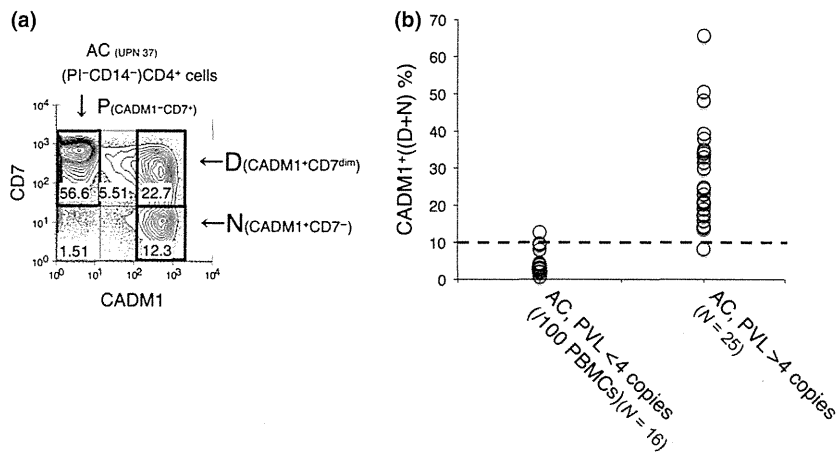
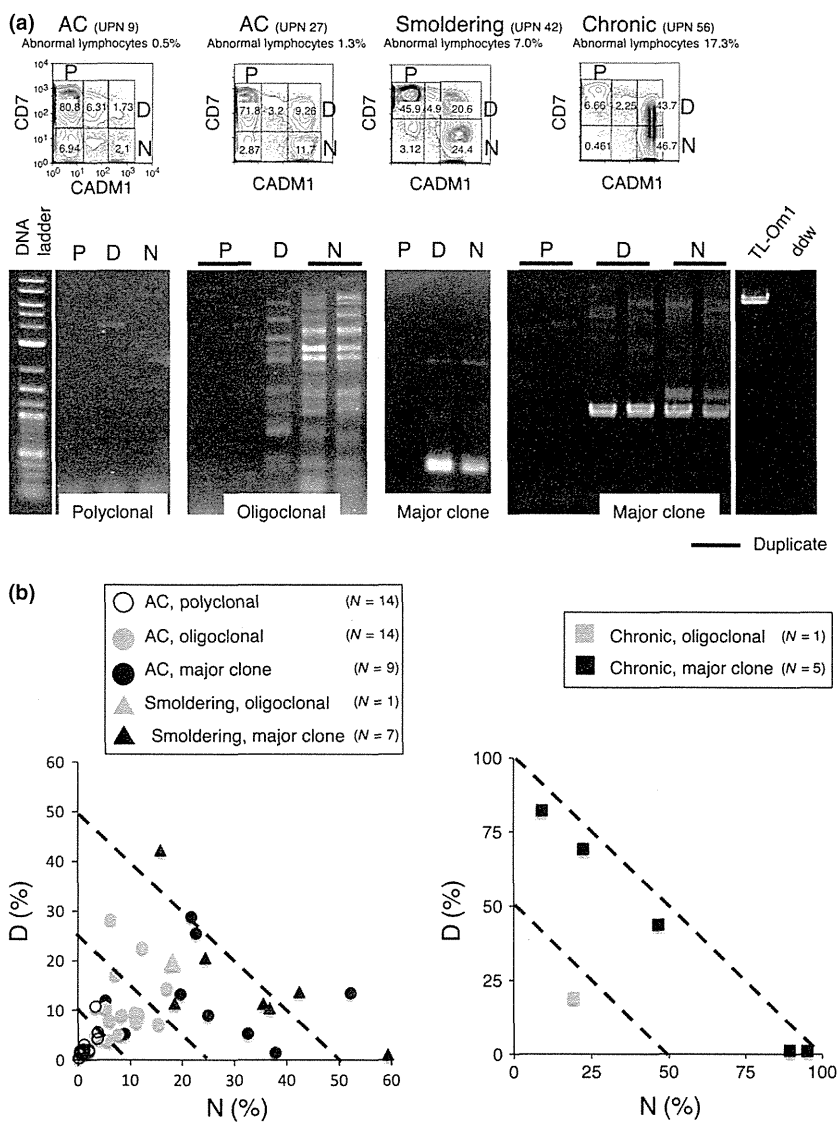


Fig. 2. Clonality analysis of the FACS-sorted subpopulations in the cell adhesion molecule 1 (CADM1) versus CD7 plot. (a) Three representative cases are shown. The three subpopulations (P, D and N) in the CADM1 versus CD7 plot were FACS-sorted and subjected to inverse long PCR. The observed band patterns were classified into “polyclonal” (left), “oligoclonal” (left middle) and “major clone” (right middle and right) states according to the number and density of the clonal bands. (b) Summary of all analyzed asymptomatic HTLV-1 carriers (AC) (left), cases of smoldering-type ATL (left) and chronic-type ATL (right). The two-dimensional plot shows the D and N subpopulation proportions for each case. The diagonal lines indicate CADM1⁺ (D + N) = 10%, 25% and 50%.



Representative cases are shown in Figure 2(a). The observed band patterns were classified into “polyclonal,” “oligoclonal” and “major clone” states according to the number and density of clonal bands. The polyclonal state was defined as barely

visible bands. The oligoclonal state was defined as a ladder-like band pattern without dominant bands, and the major clone state was defined as one or more dominant intense bands. Progression from a polyclonal state to a major clone state seemed

to correlate with increases in the CADM1⁺ (D and N) subpopulations. Figure 2(b) shows all cases analyzed by both flow cytometry and inverse long PCR and shows provisional diagonal lines indicating CADM1⁺ (D + N) = 10%, 25% and 50%. A large majority of cases distributed in the CADM1⁺ ≤ 10% area were AC with a polyclonal pattern and there were no smoldering-type ATL cases. All cases distributed in the 10% < CADM1⁺ ≤ 25% area were also AC but those with an oligoclonal pattern dominated. In the 25% < CADM1⁺ ≤ 50% area, AC and smoldering-type ATL cases were intermingled and all cases showed an oligoclonal or major clone pattern (Fig. 2b, left). Some smoldering-type ATL cases were distributed in the 50% < CADM1⁺ area and all cases showed a major clone pattern. All but one of the chronic ATL cases were distributed in the 50% < CADM1⁺ area and showed a major clone pattern (Fig. 2b, right).

Correlation of CADM1 versus CD7 profile with percentage of abnormal lymphocytes. Figure 3 shows the percentage of abnormal lymphocytes in peripheral blood from the cases in each group, classified according to CADM1⁺ (D + N) proportion. The dotted line indicates 5%, which is the borderline between AC and smoldering-type ATL according to Shimoyama's classification.^(13,14) All cases in the CADM1⁺ ≤ 10% and 10% < CADM1⁺ ≤ 25% areas are AC, as described above. No case in these groups reached the 5% line. The 25% < CADM1⁺ ≤ 50% group includes smoldering-type ATL and AC with high PVL and clonal expansion (Figs 1b,2). Intriguingly, the proportions of abnormal lymphocytes in the cases in this group were distributed around the 5% line. The 50% < CADM1⁺ group was dominated by chronic-type ATL. Most cases in this group showed a proportion of abnormal lymphocytes far above 5%.

Figure 4 shows serial changes in the percentage of abnormal lymphocytes during 39 months of observation. In all cases

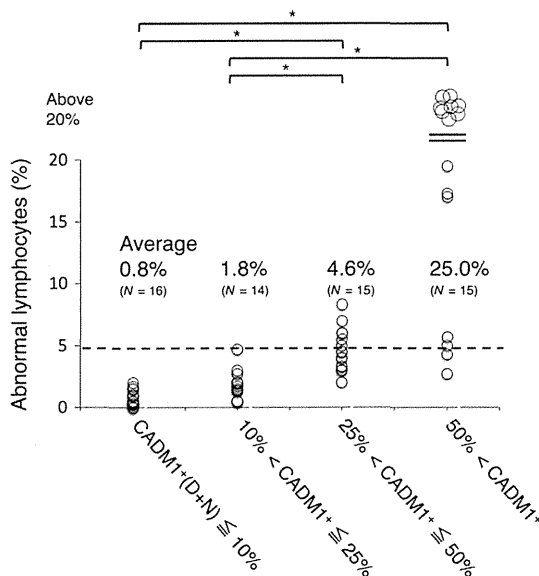


Fig. 3. Percentages of abnormal lymphocytes in groups classified by CADM1⁺ (%) in the CADM1 versus CD7 plot. All cases were classified into four groups according to CADM1⁺ (%): CADM1⁺ ≤ 10%, 10% < CADM1⁺ ≤ 25%, 25% < CADM1⁺ ≤ 50% and 50% < CADM1⁺ (see also Fig. 2b). The dotted line (5% abnormal lymphocytes) indicates the borderline between asymptomatic HTLV-1 carriers (AC) and smoldering-type ATL according to Shimoyama's classification. The 25% < CADM1⁺ ≤ 50% group includes smoldering-type ATL and AC with high PVL and major clones (see also Figs 1 and 2). **P* < 0.05. CADM1, cell adhesion molecule 1.

except for one in the CADM1⁺ ≤ 10% and 10% < CADM1⁺ ≤ 25% groups, the proportion of abnormal lymphocytes did not exceed 5%. Intriguingly, in the majority of cases in the 25% < CADM1⁺ ≤ 50% group (11 of 15 cases), the proportion of abnormal lymphocytes fluctuated on the 5% line during the observation period. In most of the cases in the 50% < CADM1⁺ group, the proportion of abnormal lymphocytes greatly exceeded 5% during the observation period.

In summary, AC and indolent ATL can be classified according to the proportion of the CADM1⁺ subpopulations ([D + N] %) in the CADM1 versus CD7 plot). The CADM1⁺ ≤ 10% group includes mainly polyclonal AC with low PVL (<4 copies per 100 PBMC). The 10% < CADM1⁺ ≤ 25% group includes oligoclonal AC with high PVL (>4 copies per 100 PBMC). The 25% < CADM1⁺ ≤ 50% group includes smoldering-type ATL and AC with major clones. Importantly, in many cases in this group the proportion of abnormal lymphocytes fluctuated around 5% (the AC/smoldering ATL borderline). The 50% < CADM1⁺ group includes chronic-type and advanced smoldering-type ATL.

Discussion

Clonally expanded HTLV-1-infected cells can be purified using cell-surface markers such as CCR4 and CD25, which have been utilized for molecular-targeted therapy.^(14,16) However, the expression levels of these markers vary among patients. A major advantage of our flow cytometry method incorporating CD3, CD7 and CADM1 is the separation of these cells with high purity from PBMC from AC as well as ATL patients, which was previously impossible.^(10,17,18) HTLV-1-infected and clonally expanding cells are enriched in the CADM1⁺ subpopulations (D and N), and progression of initial oncogenesis in these cells is reflected in the increases in D and N. In the late oncogenic process, tumor cells are generally represented by a loss of CD7 on CADM1⁺ cells in the CD4⁺ population (i.e. N is dominant in most aggressive ATL). The CADM1 versus CD7 plot consequently reflects disease progression in HTLV-1 infection.⁽¹⁰⁾

In this study, we used CADM1⁺ ([D + N] %) as an indicator of the initial oncogenic process in AC and indolent ATL. Intriguingly, the degree of dominance in D or N (i.e. N/D ratios) varied among the cases (Fig. 2b). We believe that the D and N populations are similar, but that they have unique features. For example, we previously showed that the expression of miR-31 (a microRNA with a suppressive effect on NF-κB signaling) was different between D and N cells; miR-31 was suppressed more profoundly in N than in D cells.^(10,19) It is necessary to determine how the N/D ratio contributes to the estimation of the oncogenic status of HTLV-1-infected cells.

Previous studies reported AC with various clonal statuses using methods including Southern blot analysis and PCR amplification of the HTLV-1 provirus integration sites.⁽²⁰⁻²²⁾ Although Southern blot analysis of the clonal integration of an HTLV-1 provirus is the current standard for detection of HTLV-1-infected clonal cells,⁽²³⁾ this method is not sensitive for detection of minor clones. Moreover, in most previous reports, total PBMC were used as experimental materials. Our flow cytometry method has major advantages. First, by enrichment of HTLV-1-infected cells in the CADM1⁺ subpopulations and subsequent inverse long PCR, detection of expanding clones can be more sensitive and evaluation of clonal status more accurate. Second, the CADM1 versus CD7 plot can be used to estimate the clonal status in AC as well as ATL, even

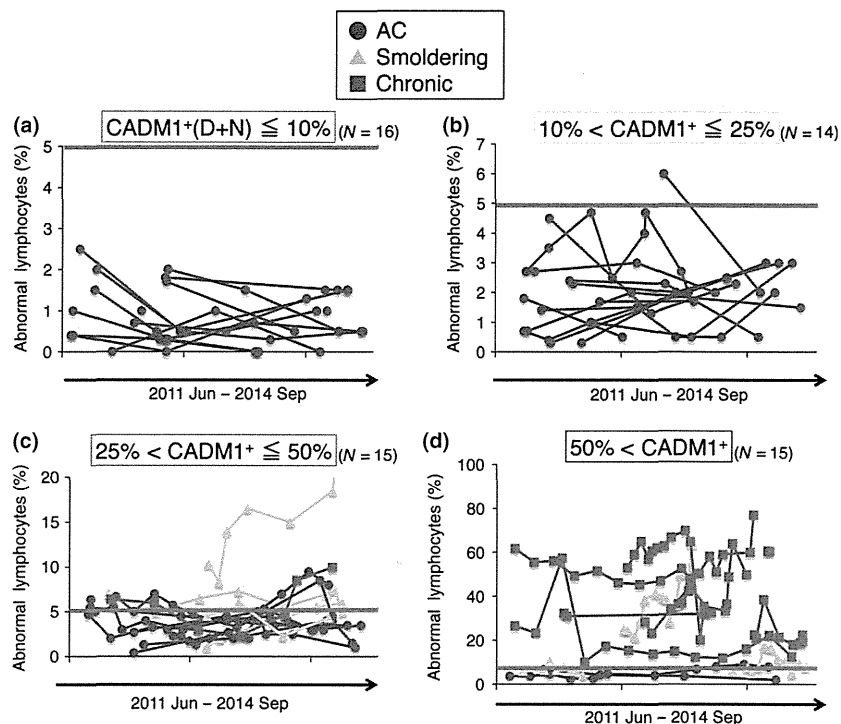


Fig. 4. Serial changes in abnormal lymphocytes (%) in groups classified by CADM1⁺ (%) in the CADM1 versus CD7 plot. (a) Data for the CADM1⁺ ≤ 10% group. The red line (5% abnormal lymphocytes) indicates the borderline between asymptomatic HTLV-1 carriers (AC) and smoldering-type ATL according to Shimoyama's classification. (b) Data for the 10% < CADM1⁺ ≤ 25% group. (c) Data for the 25% < CADM1⁺ ≤ 50% group. In many cases, the proportion of abnormal lymphocytes fluctuated around the 5% line (the AC/smoldering ATL borderline) during the observation period. (d) Data for the 50% < CADM1⁺ group. CADM1, cell adhesion molecule 1.

without further molecular analysis (Fig. 2b). Although next-generation sequencing of HTLV-1 integration sites has been developed for accurate analysis of clonality,^(24–26) our flow cytometry method (CADM1 versus CD7 plot) is simple, fast and quantitative, and will directly help in clinical management of HTLV-1-infected patients.

Using this method, we showed that AC have a variety of clonality types (Fig. 2b). Increases in the CADM1⁺ (D + N) subpopulations correlated well with clonal expansion indicated by the “polyclonal,” “oligoclonal” and “major clone” states, which were roughly divided by the CADM1⁺ = 10% and 25% lines. These data imply that oncogenic progression of each AC can be estimated by our flow cytometric analysis, and an increase in CADM1⁺ (%) in AC will mean that they are at relatively high risk of developing ATL. Although AC with high PVL exist in both the 10% < CADM1⁺ ≤ 25% and 25% < CADM1⁺ ≤ 50% groups, those in the former group are chiefly AC with oligoclonal expansion, and the latter are oligoclonal AC and AC with major clones. To reveal the relative risks of both groups will require prospective long-term observation of ATL development. Over approximately 3 years of follow up, only one AC that had a very high CADM1⁺ (%) (D + N = 65.7%, UPN 50) progressed to chronic-type ATL.

A prospective nationwide cohort study of AC by Iwanaga *et al.*⁽¹²⁾ revealed that PVL of AC have a wide range and that AC with high PVL (>4 copies/100 PBMC) are at high risk of developing ATL. As shown in Figure 1(b), CADM1⁺ [(D + N) %] in the CADM1 versus CD7 plot correlated with PVL. Almost all of the cases with PVL < 4 copies/100 PBMC were included in the CADM1⁺ ≤ 10% group, which is consistent with the finding that AC in the CADM1⁺ ≤ 10% group were polyclonal (Fig. 2b). As shown in Figure S1, when the proportions of lymphocytes and CD4⁺ cells were taken into account, the CADM1⁺ (%) for PBMC (not CD4⁺ cells) was found to approximately match the PVL. Considering that HTLV-1-infected cells are highly enriched in the CADM1⁺ population,⁽¹⁰⁾ this is a reasonable result. Therefore, our flow cytometric technique

could be utilized as a surrogate marker for PVL. Furthermore, FACS and additional molecular analyses of purified HTLV-1 clones is possible.⁽¹⁰⁾ We found that clonal status was relevant to the CADM1⁺ (%) in this study (Fig. 2), which was not possible using PVL analysis. Finally, our flow cytometric technique is simpler and easier to use for clinical testing compared to current methods for determining PVL.

The 25% < CADM1⁺ ≤ 50% group included both advanced AC and smoldering-type ATL (Fig. 2b). Their HTLV-1-infected cells in peripheral blood were oligoclonal or contained major expanding clones. The CADM1 versus CD7 profile and clonality analysis could not distinguish between AC and smoldering-type ATL patients in this group. Intriguingly, abnormal lymphocytes in the 25% < CADM1⁺ ≤ 50% group were centered on 5% (Fig. 3). We consider that many cases included in this group are the AC/smoldering ATL borderline cases classified by Shimoyama's classification. In these cases, current clinical classification depends on microscopic counting of these cells,^(13,14) although nuclear indentation in the abnormal lymphocytes is often ambiguous.⁽²⁷⁾ Observation of abnormal lymphocytes in these cases for more than 3 years (Fig. 4) revealed that many cases in the 25% < CADM1⁺ ≤ 50% group (11 of 15 cases) showed fluctuation of the abnormal lymphocyte proportion at 5% (the AC/smoldering ATL borderline). It is thus highly probable that diagnosis of such cases might differ depending on when or by which examiners they were diagnosed (e.g. a smoldering-type ATL patient with 5.5% abnormal lymphocytes might be diagnosed as an AC if the abnormal lymphocyte count at the next visit is 4.5%). To prevent confusion, the objective CADM1 versus CD7 plot will help classification of these cases. The AC and smoldering-type ATL cases included in the 25% < CADM1⁺ ≤ 50% group are believed to have similar characteristics because all of our analyses, including flow cytometry, clonality analysis and abnormal lymphocyte analysis, failed to distinguish between these two cases. However, long-term follow up is required and the clinical outcome (e.g. rate of transformation) of these cases should be

used to determine whether to include them in the same clinical category.

Finally, AC and indolent ATL will be divided into four groups based on the CADM1 versus CD7 plot. This method revealed the diversity of disease stages in AC as well as ATL, and will help us to identify advanced AC with a similar disease status to indolent ATL patients at an early stage. Some cases of smoldering ATL and AC could not be distinguished; therefore, a new clinical category that includes these cases is warranted.

Acknowledgments

We thank Mr Yuji Zaike (Clinical Laboratory, Research Hospital, Institute of Medical Science, University of Tokyo) for his excellent

technical advice. We thank Mr Keisuke Takahashi, Ms Sanae Suzuki and members of our laboratory for assistance. We are grateful to the hospital staff, who have made a commitment to providing high-quality care to all of our patients. This work was supported by Grants for Scientific Research (22591028 [K.U.], 23390250 [T.W.]) from the Ministry of Education, Culture, Sports, Science and Technology of Japan, and by Health and Labour Sciences Research Grants (H26-sink-oujitsuyuoka-ippan-013 [K.U., T.W.]) from the Ministry of Health, Labor and Welfare of Japan.

Disclosure Statement

The authors have no conflict of interest to declare.

References

- Mochizuki M, Watanabe T, Yamaguchi K *et al.* HTLV-I uveitis: a distinct clinical entity caused by HTLV-I. *Jpn J Cancer Res* 1992; **83**: 236–9.
- Yoshida M, Miyoshi I, Hinuma Y. Isolation and characterization of retrovirus from cell lines of human adult T-cell leukemia and its implication in the disease. *Proc Natl Acad Sci U S A* 1982; **79**: 2031–5.
- Osame M, Usuku K, Izumo S *et al.* HTLV-1 associated myelopathy, a new clinical entity. *Lancet* 1986; **1**: 1031–2.
- Gessain A, Cassar O. Epidemiological aspects and world distribution of HTLV-1 infection. *Front Microbiol* 2012; **3**: 388.
- Yamaguchi K, Watanabe T. Human T lymphotropic virus type-I and adult T-cell leukemia in Japan. *Int J Hematol* 2002; **76**(Suppl 2): 240–5.
- Murphy EL, Hanchard B, Figueroa JP *et al.* Modelling the risk of adult T-cell leukemia/lymphoma in persons infected with human T-lymphotropic virus type I. *Int J Cancer* 1989; **43**: 250–3.
- Iwanaga M, Watanabe T, Yamaguchi K. Adult T-cell leukemia: a review of epidemiological evidence. *Front Microbiol* 2012; **3**: 322.
- Tian Y, Kobayashi S, Ohno N *et al.* Leukemic T cells are specifically enriched in a unique CD3(dim) CD7(low) subpopulation of CD4(+) T cells in acute-type adult T-cell leukemia. *Cancer Sci* 2011; **102**: 569–77.
- Kobayashi S, Tian Y, Ohno N *et al.* The CD3 versus CD7 Plot in multicolor flow cytometry reflects progression of disease stage in patients infected with HTLV-I. *PLoS ONE* 2013; **8**: e53728.
- Kobayashi S, Nakano K, Watanabe E *et al.* CADM1 expression and step-wise downregulation of CD7 are closely associated with clonal expansion of HTLV-I-infected cells in adult t-cell leukemia/lymphoma. *Clin Cancer Res* 2014; **20**: 2851–61.
- Hisada M, Okayama A, Shioiri S, Spiegelman DL, Stuver SO, Mueller NE. Risk factors for adult T-cell leukemia among carriers of human T-lymphotropic virus type I. *Blood* 1998; **92**: 3557–61.
- Iwanaga M, Watanabe T, Utsunomiya A *et al.* Human T-cell leukemia virus type I (HTLV-1) proviral load and disease progression in asymptomatic HTLV-1 carriers: a nationwide prospective study in Japan. *Blood* 2010; **116**: 1211–9.
- Shimoyama M. Diagnostic criteria and classification of clinical subtypes of adult T-cell leukaemia-lymphoma. A report from the Lymphoma Study Group (1984–87). *Br J Haematol* 1991; **79**: 428–37.
- Tsukasaki K, Hermine O, Bazarbachi A *et al.* Definition, prognostic factors, treatment, and response criteria of adult T-cell leukemia-lymphoma: a proposal from an international consensus meeting. *J Clin Oncol* 2009; **27**: 453–9.
- Cook LB, Rowan AG, Melamed A, Taylor GP, Bangham CR. HTLV-1-infected T cells contain a single integrated provirus in natural infection. *Blood* 2012; **120**: 3488–90.
- Ishida T, Joh T, Uike N *et al.* Defucosylated anti-CCR4 monoclonal antibody (KW-0761) for relapsed adult T-cell leukemia-lymphoma: a multicenter phase II study. *J Clin Oncol* 2012; **30**: 837–42.
- Nakahata S, Saito Y, Marutsuka K *et al.* Clinical significance of CADM1/TSLC1/IgSF4 expression in adult T-cell leukemia/lymphoma. *Leukemia* 2012; **26**: 1238–46.
- Sasaki H, Nishikata I, Shiraga T *et al.* Overexpression of a cell adhesion molecule, TSLC1, as a possible molecular marker for acute-type adult T-cell leukemia. *Blood* 2005; **105**: 1204–13.
- Yamagishi M, Nakano K, Miyake A *et al.* Polycomb-mediated loss of miR-31 activates NIK-dependent NF- κ B pathway in adult T cell leukemia and other cancers. *Cancer Cell* 2012; **21**: 121–35.
- Kamihira S, Iwanaga M, Doi Y *et al.* Heterogeneity in clonal nature in the smoldering subtype of adult T-cell leukemia: continuity from carrier status to smoldering ATL. *Int J Hematol* 2012; **95**: 399–408.
- Sasaki D, Doi Y, Hasegawa H *et al.* High human T cell leukemia virus type-1 (HTLV-1) provirus load in patients with HTLV-1 carriers complicated with HTLV-1-unrelated disorders. *Virology* 2010; **7**: 81.
- Wattel E, Vartanian JP, Pannetier C, Wain-Hobson S. Clonal expansion of human T-cell leukemia virus type I-infected cells in asymptomatic and symptomatic carriers without malignancy. *J Virol* 1995; **69**: 2863–8.
- Yoshida M, Seiki M, Yamaguchi K, Takatsuki K. Monoclonal integration of human T-cell leukemia provirus in all primary tumors of adult T-cell leukemia suggests causative role of human T-cell leukemia virus in the disease. *Proc Natl Acad Sci U S A* 1984; **81**: 2534–7.
- Gillet NA, Malani N, Melamed A *et al.* The host genomic environment of the provirus determines the abundance of HTLV-1-infected T-cell clones. *Blood* 2011; **117**: 3113–22.
- Cook LB, Melamed A, Niederer H *et al.* The role of HTLV-1 clonality, proviral structure, and genomic integration site in adult T-cell leukemia/lymphoma. *Blood* 2014; **123**: 3925–31.
- Firouzi S, Lopez Y, Suzuki Y *et al.* Development and validation of a new high-throughput method to investigate the clonality of HTLV-1-infected cells based on provirus integration sites. *Genome Med* 2014; **6**: 46.
- Tsukasaki K, Imaizumi Y, Tawara M *et al.* Diversity of leukaemic cell morphology in ATL correlates with prognostic factors, aberrant immunophenotype and defective HTLV-1 genotype. *Br J Haematol* 1999; **105**: 369–75.

Supporting Information

Additional supporting information may be found in the online version of this article:

Fig. S1. Correlation of proviral load (PVL) and CADM1⁺ (%) in the CADM1 versus CD7 plot.

第4章 特異的神経感染症

ヒトT細胞白血病ウイルス1型関連脊髄症

要旨

HTLV-1 関連脊髄症 (HAM) は、ヒトT細胞白血病ウイルス1型 (HTLV-1) 感染に起因する、慢性進行性の両下肢痙性麻痺、感覚障害、膀胱直腸障害を呈する神経難病である。現時点で根本的治療はなく、ステロイドやインターフェロン α (IFN α) による脊髄の炎症の制御が治療の主流であるが、症状に個人差が大きく、疾患活動性を見極めた治療が重要であるため、発症早期の診断が望まれる。また近年、大都市圏でも患者数の増加が見られるため、痙性麻痺を診たときの鑑別疾患としても、頭にとどめていただきたい。

はじめに

HTLV-1 関連脊髄症 (HAM) は、ヒトT細胞白血病ウイルス1型 (HTLV-1) の感染者 (キャリア) の一部に発症する、進行性の脊髄障害を特徴とする神経難病である。1986年に納らにより1つの疾患単位として提唱され¹⁾、2009年度からは我が国の難治性疾患克服研究事業の対象疾患 (いわゆる難病) に認定されている。

疫学

HTLV-1 キャリアは全国で約110万人存在するが、その約5%に成人T細胞白血病 (ATL)、約0.3%にHAMが発症すると推定されている²⁾。感染者やHAM、ATL患者は、西日本を中心に全国に分布し、特に九州・四国・沖縄に多い。しかし最近の全国疫学調査では、全国のHAM患者数は約3,000人と推定され、関東などの大都市圏で患者数が増加していることが明らかになってきた。

●キーワード

HTLV-1
HAM

HTLV-1の感染経路として、主として母乳を介する母子感染と、輸血、性交渉による水平感染が知られているが、1986年11月より献血時の抗HTLV-1抗体のスクリーニングが開始され、以後、輸血後

発症はない。発症は中年以降の成人が多いが（平均発症年齢は40歳代）、10歳代、若年発症例も存在する。男女比は1:2と女性に多い。

診断と鑑別診断

表1 HTLV-1 関連脊髄症 (HAM) 初期症状

- ・何となく歩きにくい、両下肢のつっぱり感、足がもつれる、つまずく、走ると転びやすい、などの歩行障害に関する症状
- ・排尿障害や便秘も、早期から自覚されることが多く、尿閉や頻尿、繰り返す膀胱炎で泌尿器科を受診し、HAMと診断されることもある
- ・まれに、持続する両下肢のしびれ感、痛みなどを早期から認めることがある

HAMは希少疾患ゆえに、発症初期の段階で鑑別にあがりにくい。HAMは早期に診断し治療介入することが重要であるため、見逃さないよう注意が必要である。症状も多彩であるため、整形外科や泌尿器科を受診する患者も多い。表1のような患者を診たら、HAMという疾患を思い浮かべ、HAMを疑ったらすぐに神経内科医への紹介を考慮して

ほしい。

HAMの診断には、まず血清中の抗HTLV-1抗体の有無をEIA法またはPA法でスクリーニングし、陽性の場合にはウエスタンブロット法で確認、感染を確定する。感染が確認されたら髄液検査を施行し、髄液の抗HTLV-1抗体が陽性の場合、ほかのミエロパチーを来す脊髄圧迫病変、脊髄腫瘍、多発性硬化症、視神経脊髄炎などを鑑別したうえで、HAMと確定診断する⁹⁾。

症状・経過

臨床症状の中核は、緩徐進行性の両下肢痙性不全麻痺で、両下肢の筋力低下と痙性による歩行障害を示す。初期症状は、歩行の違和感、足のしびれ、つっぱり感、足がもつれる、転びやすい、などであるが、多くは進行し、片手杖、両手杖、さらに車椅子が必要となる。重症例では下肢の完全麻痺や体幹の筋力低下による座位保持困難により、寝たきりになる場合もある。感覚障害は約6割に認められ、下半身の触覚や温痛覚の低下、持続するしびれ感や痛みなどが見られるが、特に痛みを伴う場合は、QOL低下の主要な原因となる⁹⁾。

自律神経症状は高率に見られ、特に排尿困難、頻尿、便秘などの膀胱直腸障害は、病初期より見られる。また、進行例では起立性低血圧や下半身の発汗障害なども認められ、発汗低下によるうつ熱のため、夏場に微熱、倦怠感が続き、適切な室温管理が必要となる。そのほか、